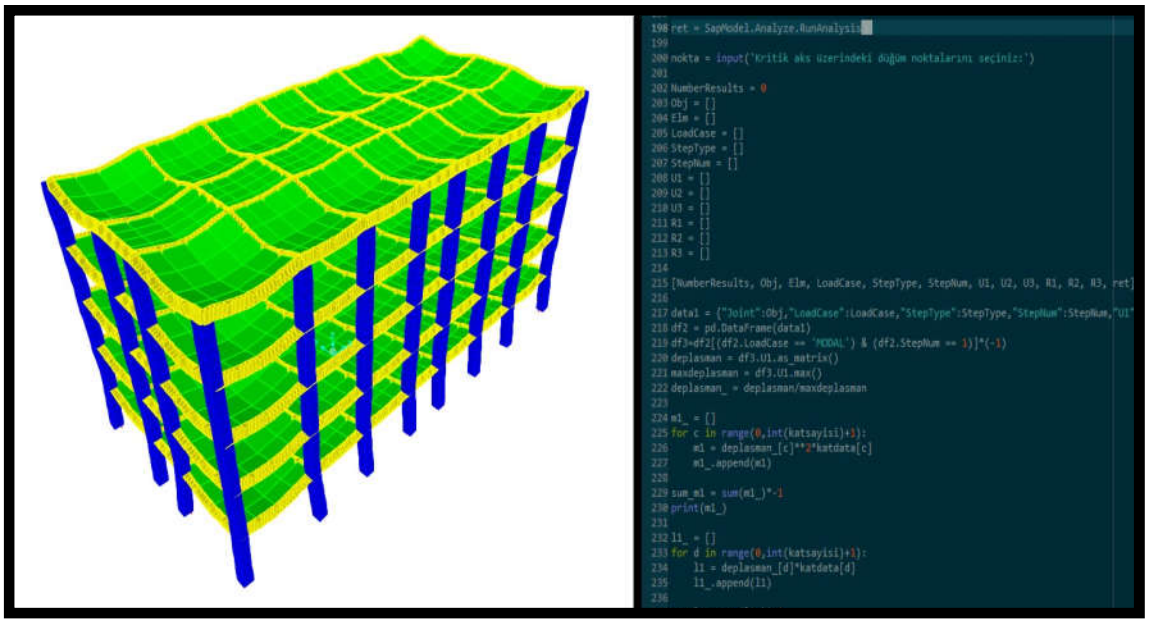

Oğuzhan Usta
Gökhan Altıntaş

Parametric Design and Investigation of Base Isolators Using the Script Developed on SAP2000 OAPI

Parametric Design and Investigation of Base Isolators Using the Script Developed on SAP2000 OAPI

Oğuzhan Usta
Gökhan Altıntaş

MCBU CIVIL ENGINEERING REPORTS

MCBUCIVILENG.R-2020.1

Report No: MCBUCIVILENG.R-2020.1
Release Year: 2020

MANİSA CELAL BAYAR ÜNİVERSİTESİ İNŞAAT MÜHENDİSLİĞİ

Report Title
Parametric Design and Investigation of Base Isolators Using the Script Developed on SAP2000 OAPI

Author(s)
Oğuzhan Usta, Gökhan Altıntaş

Report Identification Code
MCBUCIVILENG.R-2020.1

Abstract

Earthquakes are one of the frequently observed natural disasters that can have very devastating consequences. In the absence of measures that should be taken in accordance with the effects of the natural disaster in question, it is highly possible to encounter undesirable situations. Many different methods have been tried and applied until today in order to prevent damages that may occur due to earthquakes. One of the current methods used is to provide seismic isolation between the building and the ground.

The main purpose of seismic isolation works is to reduce the interaction between the building and the ground and to ensure that the building is not affected by ground movements.

Many different types of seismic isolators are used in earthquake resistant building applications. One of these isolator types is lead-core rubber isolator systems that are widely used today.

In this study, the behavior of a structure with lead-core rubber isolators provided seismic isolation was investigated for various earthquake records using the SAP2000 analysis program and the software developed specifically for this study in the Python programming language operating through The Open Application Programming Interface (OAPI).

In addition, in this study, the effects of the changes in the various properties of the base isolators on the behavior of the structure under the effect of selected earthquakes were analyzed parametrically using the developed software.

Keywords
Isolation, Lead Rubber Bearing, Python, SAP2000, OAPI, LRB, Base Isolation, Earthquake, Damping

Pages
49

Sponsor(s) / Funds / Support(s)
-

Report Information
Independent Research Project

Acceptance Date 12 November, 2020

Acceptance Committee (5)

Assoc. Prof. Dr. Ali Demir
Assoc. Prof. Erkan Doğan
Assoc. Prof. Dr. Tuğrul Erdem
Assoc. Prof. Dr. Engin Gücüyen
Dr. Mehmet B. Bozkurt

Contact Addresses & Affiliations
Oğuzhan Usta (MCBU)
Email(s): oguzhanusta.10@gmail.com
Address: Süleyman Demirel Mahallesi, 1104 Sokak, No:1 Kat:3 Daire:5 Ödemiş / İzmir Turkey
Prof. Dr. Gökhan Altıntaş (MCBU)
Email(s): gokhanaltintas@gmail.com gokhan.altintas@cbu.edu.tr
Address: Manisa Celal Bayar Üniversitesi, İnşaat Mühendisliği Bölümü, Mühendislik Fakültesi B Blok, Şehit Prof. Dr. İlhan Varank Kampüsü 45140, Yunusemre / Manisa Turkey

Abstract

Earthquakes are one of the frequently observed natural disasters that can have very devastating consequences. In the absence of measures that should be taken in accordance with the effects of the natural disaster in question, it is highly possible to encounter undesirable situations. Many different methods have been tried and applied until today in order to prevent damages that may occur due to earthquakes. One of the current methods used is to provide seismic isolation between the building and the ground.

The main purpose of seismic isolation works is to reduce the interaction between the building and the ground and to ensure that the building is not affected by ground movements.

Many different types of seismic isolators are used in earthquake resistant building applications. One of these isolator types is lead-core rubber isolator systems that are widely used today.

In this study, the behavior of a structure with lead-core rubber isolators provided seismic isolation was investigated for various earthquake records using the SAP2000 analysis program and the software developed specifically for this study in the Python programming language operating through The Open Application Programming Interface (OAPI).

In addition, in this study, the effects of the changes in the various properties of the base isolators on the behavior of the structure under the effect of selected earthquakes were analyzed parametrically using the developed software.

Keywords: Isolation, Lead Rubber Bearing, Python, SAP2000, OAPI, LRB, Base Isolation, Earthquake, Damping

TABLE OF CONTENTS

LIST OF TABLES

LIST OF FIGURES

Introduction

Earthquakes bring with them a multitude of undesirable effects and events. Especially with the settlement of human beings, more permanent structures have begun to be built and the unwanted effects of earthquakes have started to be observed more on these structures. People's efforts to protect buildings from these undesirable effects of earthquakes are not much new. Various applications based on the principle of creating layers separating buildings from the ground and preventing the structure-ground relationship date back to today's engineering applications.
The underlying idea of base isolation works is based on a fairly simple principle. Different ideas have been proposed and used to separate the structures from the ground, such as using rollers, layers of sand or similar materials. In this way, it is aimed that possible ground movements affect the structure as little as possible. Base-isolation systems aim to attenuate the effect of horizontal components of ground acceleration by using structural elements with a relatively horizontal rigidity between the structure and the ground. (Kelly, 2004) Although the first foundation isolation patents began in the 1800s and seismic isolation samples were applied in the early 1900s (for example, the Tokyo Imperial Hotel), it took the 1970s for the "seismic isolation" issue to become an integral part of structural engineering. Even in the first applications in bridges, energy dissipation and damping are provided as well as preserving flexibility. Lead-core rubber isolators were invented in the 1970s, and these systems are based on the idea of providing both flexibility and damping together in one unit. (Kelly, 2001)
The said lead-core rubber isolator system allows the structure to oscillate at a much lower frequency than both the base frequency of the non-isolated state and the dominant frequencies of ground motion.

Some of the widely used seismic isolator systems worldwide are:

- Elastomer Based Isolators
- Low-Damping Natural & Synthetic Rubber Bearings
- High Damping Natural Rubber Isolators (HDNR)
- Sliding Base Isolation System
- Friction Pendulum Bearing
- Triple or Double Concave Friction Pendulum Bearings
- Spring Vibration Isolation
- Lead Rubber Bearings

In this study, *"Lead Rubber Bearings (LRB)"* were used.

Lead Rubber Bearings (LRB)

The lead-rubber bearing (LRB) was invented in 1975 by W. H. Robinson in New Zealand (Skinner et al., 1993; Kelly, 2004; Robinson and Tucker, 1977, 1983).

LRBs are generally made of low-damping (unfilled) elastomers (with shear modules ranging from 65 to 100 psi at 100% shear strain) and lead cores with diameters ranging from 15% to 33% of the bearing's bonded diameter. The elastomer supplies the isolation component and the lead core supplies the energy dissipation or damping component. (Constantinou et al., 2007)

Generally, a lead rubber isolator consists of a low-damping elastomer and one (typically) or more (less

common) lead core. The cross-sectional view of a lead rubber isolator is shown in Figure 1. (Constantinou et al. 2007b)

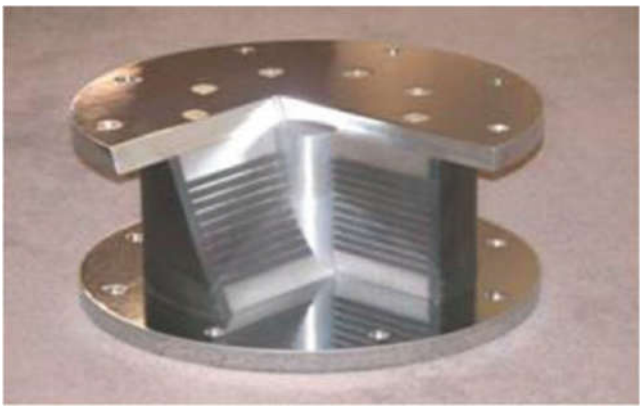

Figure 1: Sectional view of lead-rubber bearing. (Constantinou et al. 2007b)

Elastomer rubber layers function as an "isolating" component (ie, stiffness and structural frequency reduction). Steel plates help vertical load support. The lead core mainly functions as the "damping" component. (Constantinou et al. 2007b)

The lead core provides successful energy absorption capacity under limited conditions. These conditions can be achieved by making the connection slightly longer than the height of the rubber isolator and attaching the upper and lower flange plates to the rubber bearing end plates by means of countersunk bolts. Then, the connection is tightened upon the bolting of the flange plates to the end plates; expands laterally and wedges into the rubber layers between shim plates. (Constantinou et al. 2007b)

Base isolation codes represent damping arising from all sources as equivalent viscous damping, damping which is a function of velocity. Most types of isolators provide damping which is classified as hysteretic, damping which is a function of displacement. (Kelly, 2001) Where A_h is the area of the hysteresis loop and K_{eff} is the effective stiffness of the isolator at displacement Δ, as shown in Figure 2. (Kelly, 2001)

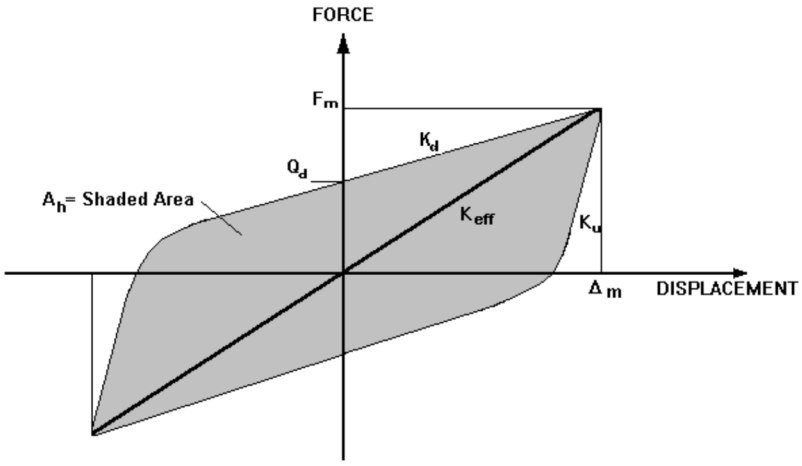

Figure 2: Hysteresis loop in lead-rubber bearings. (Kelly, 2001)

UBC 97 – General Definitions

The following section includes some technical definitions from UBC97. (Uniform Building Code, 1997)

- ***Design-Basis Earthquake:*** Earthquake expected to be overcome within 50 years with 10 percent probability
- ***Maximum Capable Earthquake:*** Maximum level of earthquake ground shaking that may ever be expected at the building site within the known geological framework. In Seismic Zones 3 and 4, this intensity may be taken as the level of earthquake ground motion that has a 10 percent probability of being exceeded in a 100-year time period.
- ***Effective Damping:*** The value of equivalent viscous damping corresponding to energy dissipated during cyclic response of the isolation system.
- ***Effective Stiffness:*** The value of the lateral force in the isolation system, or an element thereof, divided by the corresponding lateral displacement.
- ***Total Design Displacement:*** The design-basis earthquake lateral displacement, including additional displacement due to actual and accidental torsion, required for design of the isolation system, or an element thereof.
- **Total Maximum Displacement:** The maximum capable earthquake lateral displacement, including additional displacement due to actual and accidental torsion, required for verification of the stability of the isolation system, or elements thereof, design of building separations, and vertical load testing of isolator unit prototypes.
- ***Effective Period:*** Effective period, in seconds, of seismic-isolated structure at the design displacement in the direction under consideration, as prescribed by Formula (58-2) in UBC-97.
- ***Isolation System:*** The collection of structural elements that includes all individual isolator units, all structural elements that transfer force between elements of the isolation system, and all connections to other structural elements. The isolation system also includes the wind-restraint system if such a system is used to meet the design requirements of this section.

UBC 97- Detection of Seismic Coefficient

The definitions in UBC-97 and Güner's study were used to calculate the seismic coefficients in the code.(Güner, 2012; Uniform Building Code, 1997)

- ***Detection of Seismic Zone Coefficient:*** Seismic zone and seismic zone coefficient, Z can be found with the tables given in UBC-97 and Table 1 in this study.
- ***Detection of Soil Profile Type:*** Soil Profile Types, S_A, S_B, S_C, S_D and S_E are defined in Table 16-J in UBC-97 and Table 2 in this study. Soil Profile Type S_F is defined as soils requiring site-specific evaluation as follows:

  1. Soils vulnerable to potential failure or collapse under seismic loading, such as liquefiable soils, quick and highly sensitive clays, and collapsible weakly cemented soils.

  2. Peats and/or highly organic clays, where the thickness of peat or highly organic clay exceeds 3048 mm.

  3. Very high plasticity clays with a plasticity index, PI > 75, where the depth of clay exceeds 7620 mm.

  4. Very thick soft/medium stiff clays, where the depth of clay exceeds 36 576 mm.

- ***Finding Seismic Source Type:*** In UBC-97, seismic source types were made for different regions. These resource types are determined according to the Table 3.
- ***Finding Near-Source Factors:*** Depending on the seismic source type, the Table 4-5 below is used to find the seismic source multipliers ($N_a$and N_v).
- ***Calculation of the Power of Design Earthquake:*** This power is equal to the product of Z and N_v.

- ***Detection of Maximum Capable Earthquake Response Coefficient:*** The numerical coefficient for the maximum capacity earthquake response can be found in the Table 6 below.
- ***Calculation of Seismic Coefficients:*** C_a and C_v, the seismic coefficients, can be calculated with Table 7-8.
- C_{VM} and C_{AM} values in Table 9-10 are found using the $M_M Z N_a$ and $M_M Z N_v$ values.
- ***Detection of Structure Behavior Coefficient (R):*** It is considered appropriate to take R=2 for systems with seismic isolation.

Table 1: SEISMIC ZONE FACTOR, Z (Table 16 – I)

ZONE	1	2A	2B	3	4
Z	0,075	0,15	0,20	0,30	0,40

Table 2: SOIL PROFILE TYPES (Table 16 – J)

Soil Profile Type	**Soil Profile Name/Generic Description**	**Average Soil Properties for Top 100 Feet (30 480 mm) of Soil Profile**		
		Shear Wave Velocity, V_s feet/second (m/s)	**Standard Penetration Test, $\bar{N}$ [or $\bar{N}_{CH}$ for cohesionless soil layers] (blows/foot)**	**Undrained Shear Strength, $\bar{s}_u$ psf (kPa)**
S_A	Hard Rock	> 5000 (1500)	–	–
S_B	Rock	2500 to 5000 (760 to 1500)		
S_C	Very Dense Soil and Soft Rock	1200 to 2500 (360 to 760)	> 50	>2000 (100)
S_D	Stiff Soil Profile	600 to 1200 (180 to 360)	15 to 50	1000 to 2000 (50 to 100)
S_E[1]	Stiff Soil Profile	< 600 (180)	< 15	< 1000 (50)
S_F	Soil Requiring Site-specific Evaluation. See Section 1629.3.1 in UBC-97.			

1-Soil Profile Type S_E also includes any soil profile with more than 10 feet (3048 mm) of soft clay defined as a soil with a plasticity index, PI > 20, $w_{mc} \geq 40$ percent and su < 500 psf (24 kPa). The Plasticity Index, PI, and the moisture content, w_{mc}, shall be determined in accordance with approved national standards.

Table 3: SEISMIC SOURCE TYPE[1] (Table 16 – U)

Seismic Source Type	Seismic Source Description	Seismic Source Description[2]	
		Maximum Moment Magnitude, M	Slip Rate, SR (mm/year)
A	Faults that are capable of producing large magnitude events and that have a high rate of seismic activity	M ≥ 7,0	SR ≥ 5
B	All faults other than Types A and C	M ≤ 7,0	SR < 5
		M < 7,0	SR < 2
		M ≥ 6,5	SR< 2
C	Faults that are not capable of producing large magnitude earthquakes and that have a relatively low rate of seismic activity	M < 6,5	SR ≤ 2

1-Subduction sources shall be evaluated on a site-specific basis.
2-Both maximum moment magnitude and slip rate conditions must be satisfied concurrently when determining the seismic source type.

Table 4: NEAR-SOURCE FACTOR, N_a^1 (Table 16 – S)

Seismic Source Type	Closest Distance To Known Seismic Source[2,3]		
	≤ 2 km	5km	≥ 10 km
A	1,5	1,2	1,0
B	1,3	1,0	1,0
C	1,0	1,0	1,0

1-The Near-Source Factor may be based on the linear interpolation of values for distances other than those shown in the table.
2-The location and type of seismic sources to be used for design shall be established based on approved geotechnical data (e.g., most recent mapping of active faults by the United States Geological Survey or the California Division of Mines and Geology).
3-The closest distance to seismic source shall be taken as the minimum distance between the site and the area described by the vertical projection of the source on the surface (i.e., surface projection of fault plane). The surface projection need not include portions of the source at depths of 10 km or greater. The largest value of the Near-Source Factor considering all sources shall be used for design.

Table 5: NEAR-SOURCE FACTOR, N_v^1 (Table 16 – T)

Seismic Source Type	Closest Distance To Known Seismic Source[2,3]			
	≤ 2 km	5km	10 km	≥15 km
A	2,0	1,6	1,2	1,0
B	1,6	1,2	1,0	1,0
C	1,0	1,0	1,0	1,0

1-The Near-Source Factor may be based on the linear interpolation of values for distances other than those shown in the table.
2-The location and type of seismic sources to be used for design shall be established based on approved geotechnical data (e.g., most recent mapping of active faults by the United States Geological Survey or the California Division of Mines and Geology).
3-The closest distance to seismic source shall be taken as the minimum distance between the site and the area described by the vertical projection of the source on the surface (i.e., surface projection of fault plane). The surface projection need not include portions of the source at depths of 10 km or greater. The largest value of the Near-Source Factor considering all sources shall be used for design.

Table 6: MAXIMUM CAPABLE EARTHQUAKE RESPONSE COEFFICIENT, M_M (Table A 16 – D)

Design Basis Earthquake Shaking Intensity, ZN_v	Maximum Capable Earthquake Response Coefficient, M_M
0,075	2,67
0,15	2,0
0,20	1,75
0,30	1,50
0,40	1,25
≥ 0,50	1,20

Table 7: SEISMIC COEFFICIENT, C_a (Table 16 – Q)

Soil Profile Type	Seismic Zone Factor, Z				
	Z = 0,075	Z = 0,15	Z = 0,20	Z = 0,30	Z = 0,40
S_A	0,06	0,12	0,16	0,24	$0{,}32N_a$
S_B	0,08	0,15	0,20	0,30	$0{,}40N_a$
S_C	0,09	0,18	0,24	0,33	$0{,}40N_a$
S_D	0,12	0,22	0,28	0,36	$0{,}44N_a$
S_E	0,19	0,30	0,34	0,36	$0{,}36N_a$
S_F	See Footnote 1				

1-Site-specific geotechnical investigation and dynamic site response analysis shall be performed to determine seismic coefficients for Soil Profile Type S_F.

Table 8: SEISMIC COEFFICIENT, C_v (Table 16 – R)

Soil Profile Type	Seismic Zone Factor, Z				
	Z = 0,075	Z = 0,15	Z = 0,20	Z = 0,30	Z = 0,40
S_A	0,06	0,12	0,16	0,24	$0{,}32N_v$
S_B	0,08	0,15	0,20	0,30	$0{,}40N_v$
S_C	0,13	0,25	0,32	0,45	$0{,}56N_v$
S_D	0,18	0,32	0,40	0,54	$0{,}64N_v$
S_E	0,26	0,50	0,64	0,84	$0{,}96N_v$
S_F	See Footnote 1				

1-Site-specific geotechnical investigation and dynamic site response analysis shall be performed to determine seismic coefficients for Soil Profile Type S_F.

Table 9: SEISMIC COEFFICIENT, C_{AM}[1] (Table A 16 – F)

Soil Profile Type	Maximum Capable Earthquake Shaking Intensity, $M_M ZN_a$				
	$M_M ZN_a = 0{,}075$	$M_M ZN_a = 0{,}15$	$M_M ZN_a = 0{,}20$	$M_M ZN_a = 0{,}30$	$M_M ZN_a \geq 0{,}40$
S_A	0,06	0,12	0,16	0,24	$0{,}8 M_M ZN_a$
S_B	0,08	0,15	0,20	0,30	$1{,}0 M_M ZN_a$
S_C	0,09	0,18	0,24	0,33	$1{,}0 M_M ZN_a$
S_D	0,12	0,22	0,28	0,36	$1{,}1 M_M ZN_a$
S_E	0,19	0,30	0,34	0,36	$0{,}9 M_M ZN_a$
S_F	See Footnote 2				

1-Linear interpolation may be used to determine the value of C_{AM} for values of $M_M ZN_a$ for other than those shown in the table.
2-Site-specific geotechnical investigation and dynamic site response analysis shall be performed to determine seismic coefficients for soil.

Table 10: SEISMIC COEFFICIENT, C_{VM}[1] (Table A 16 – G)

Soil Profile Type	Maximum Capable Earthquake Shaking Intensity, $M_M ZN_v$				
	$M_M ZN_v = 0{,}075$	$M_M ZN_v = 0{,}15$	$M_M ZN_v = 0{,}20$	$M_M ZN_v = 0{,}30$	$M_M ZN_v \geq 0{,}40$
S_A	0,06	0,12	0,16	0,24	$0{,}8 M_M ZN_v$
S_B	0,08	0,15	0,20	0,30	$1{,}0 M_M ZN_v$
S_C	0,13	0,25	0,32	0,45	$1{,}4 M_M ZN_v$
S_D	0,18	0,32	0,40	0,54	$1{,}6 M_M ZN_v$
S_E	0,26	0,50	0,64	0,84	$2{,}4 M_M ZN_v$
S_F	See Footnote 2				

1-Linear Interpolation may be used to determine the value of C_{VM} for values of $M_M ZN_v$ for other than those shown in the table.
2-Site-specific geotechnical investigation and dynamic site response analysis shall be performed to determine seismic coefficients for soil.

UBC97 – Calculation of Isolator Parameters

UBC-97 and Güner's study were used to calculate the isolator parameters that comply with the regulation. (Güner, 2012; Uniform Building Code, 1997)

Target period and material properties

Period values between 2 and 3 seconds are desired values for the vibration period of the isolation system. Elasticity module E, shear modulus G, and maximum shear deformation γ_{max} differ depending on the type of isolator selected.

Design and calculation of maximum displacement

The isolation system shall be designed and constructed to withstand minimum lateral earthquake displacements acting in the direction of each of the main horizontal axes of the structure in accordance with the following formula:

$$d_D = (g \times C_V D \times T_D)/(B_D \times 4\pi^2) \qquad \textbf{(Eq. 1)}$$

Here, g is gravitational acceleration, C_VD seismic coefficient, T_D design period, B_D damping coefficient.

The value of B_D is calculated using Table 11. When calculating the maximum displacement of the isolation system in the horizontal direction, C_{VM} instead of C_{VD}, T_M instead of T_D and B_M instead of B_D.

$$d_M = (g \times C_V M \times T_M)/(B_M \times 4\pi^2) \qquad \textbf{(Eq. 2)}$$

Calculation of effective horizontal stiffness

The horizontal stiffness of a single isolator in the isolation system in the direction discussed is calculated as follows.

$$K_H = K_eff = w/g \times [(2\pi/T_D)]^2 \quad \textbf{(Eq. 3)}$$

W is the normal force acting on a single isolator and is calculated by dividing the total weight of the structure by the number of isolators.

Calculation of the amount of energy absorbed in each cycle

The energy absorbed by the seismic isolator for each cycle can be calculated with the formula below. This value is used to calculate the characteristic strength Q_d.

$$W_D = 2\pi \times K_eff \times (d_D)^2 \times \beta_eff \quad \textbf{(Eq. 4)}$$

Calculation of characteristic strength

The characteristic strength of a single isolator is calculated as follows, as $\underline{d_Y}$ is the displacement in the flow state, since this value is too small compared to the d_D design displacement.

$$W_D = 4 \times Q_d \times (d_D - d_Y) \quad \textbf{(Eq. 5)}$$

$$Q_D = W_D/(4 \times d_D) \quad \textbf{(Eq. 6)}$$

Calculation of yield displacement

The displacement in the case of shear yielding where the change in the horizontal stiffness of the seismic isolator occurs is calculated as follows. K_u is the pre-yield stiffness, and K_d is the post-yield stiffness.

$$d_y = Q_D/(K_u \times K_d) \quad \textbf{(Eq. 7)}$$

$$K_u = 10 \times K_d \quad \textbf{(Eq. 8)}$$

$$d_y = Q_d/(9 \times K_d) \quad \textbf{(Eq. 9)}$$

$$K_d = K_eff - (Q_d/d_d) \quad \textbf{(Eq. 10)}$$

Calculation of lead core cross-section

The characteristic strength of the lead core cross-sectional area required in a single isolator is calculated by dividing the lead to yield stress (f_y).

$$A_{pb} = Q_d/f_y \quad \textbf{(Eq. 11)}$$

Horizontal stiffness provided by lead core

The horizontal stiffness provided by the lead core can be calculated with the formula below.

$$K_{pb} = Q_d/d_D \quad \textbf{(Eq. 12)}$$

Rigidity provided by the rubber part

The stiffness provided by the rubber part is found by removing the stiffness provided by the lead core from the total lateral stiffness of the isolator.

$$K_{rub} = K_d = K_H - K_{pb} \quad \textbf{(Eq. 13)}$$

Calculation of cross-section of the rubber part

After determining the diameter of the isolator and the required lead core diameter, the difference between both cross-sectional areas gives the required rubber cross-section, A_{rub}.

Calculation of the required total rubber thickness

The total required rubber thickness, including the G shear modulus, is calculated as follows.

$$K_{rub} = (G \times A_{rub})/K_{rub} \quad \textbf{(Eq. 14)}$$

Calculation of the shape factor

After determining the thickness of a single rubber layer, the shape factor can be calculated. t value should be in the range specified below.

$$\theta \leq 80 \leq \theta/40 \quad \textbf{(Eq. 15)}$$

Here θ is the diameter of the isolator. The shape factor is calculated as follows.

$$S = Loaded\ area/Unloaded\ area = Disk\ space/Lateral\ space = (\pi \times \theta^2/4) \div (\pi \times \theta \times t) \quad \textbf{(Eq. 16)}$$

$$S = \theta/(4 \times t) \quad \textbf{(Eq. 17)}$$

Calculation of the vertical stiffness of the isolator

Vertical rigidity is calculated as E_c pressure elasticity module as follows.

$$K_v = (E_c \times A_s)/t_r = (6 \times G \times S^2)/t_r \quad \textbf{(Eq. 18)}$$

Calculation of yield strength

Yield strength can be calculated with the formula below.

$$F_y = Q_d + K_d \times d_y \quad \textbf{(Eq. 19)}$$

Calculation of shape deformations

The deformations in the horizontal and vertical can be calculated as follows.

$$y_v = 6 \times S \times \varepsilon_z \quad \textbf{(Eq. 20)}$$

$$\varepsilon_z = \Delta t/h_{total} \quad \textbf{(Eq. 21)}$$

$$\Delta_t = W/k_v \quad \textbf{(Eq. 22)}$$

In these formulas, Δ_t is the vertical displacement, and h_{top} is the height of the isolator.

Calculation of slip shape deformations

Horizontal;

$$y_s = \tau/G = V_D/(A_s \times G) = (K_d \times d_d)/(A_s \times G) \quad \textbf{(Eq. 23)}$$

The maximum deformation is;

$$y_{max} = y_v \times y_s \quad \textbf{(Eq. 24)}$$

Common area calculations

The common area in case of slip can be calculated as follows.

$$A' = A_s[1 - 2/\pi(\theta + sin\theta \times cos\theta)]A' = A_s[1 - 2/\pi(\theta + sin\theta \times cos\theta)]$$

s **(Eq. 25)**

$$sin\theta = d_D/DA' = A_s[1 - 2/\pi(\theta + sin\theta \times cos\theta)] \quad \textbf{(Eq. 26)}$$

Calculation of critical buckling load

The load that a single isolator can carry without causing buckling is calculated by the formula below.

$$P_{critical} = \sqrt{((A \times G \times \pi^2 \times E_c \times I)/(3t^2))} \quad \textbf{(Eq. 27)}$$

$$I = (\pi/4) \times (\theta/2)^4 \quad \textbf{(Eq. 28)}$$

Table 11: DAMPING COEFFICIENTS, B_D AND B_M (Table A 16 – C)

Effective Damping β_D or β_M (percentage of critical)[1,2]	B_D or B_M Factor
≤ 2	0,8
5	1,0
10	1,2
20	1,5
30	1,7
40	1,9
≥ 50	2,0

1-The damping coefficient shall be based on the effective damping of the isolation system determined in accordance with the requirements of Section 1665.5.

2-The damping coefficient shall be based on linear interpolation for effective damping values other than those given.

Investigation of Base Isolators by Software Programming

SAP2000 OAPI

The CSI Application Programming Interface (API) is a tool that allows users to automate many processes needed to create, analyze, design models, and achieve customized analysis and design results. It also allows users to connect programs such as SAP2000 or ETABS with third-party software and provides a way to exchange two-way model information with other programs.

It is possible to create a spreadsheet, add-on or third-party application that can interface with CSI software with a little programming knowledge. The API is compatible with most common programming languages, including Visual Basic for Applications (VBA), VB.NET, C #, C ++, Visual Fortran, Python and MATLAB. ("Application Programming Interface | Computers and Structures, Inc. | csiamerica.com")

Python

Technically, Python is primarily an object-oriented, high-level programming language with integrated dynamic semantics (meaningful) for web and application development. It is extremely attractive in the field of Rapid Application Development because it offers dynamic writing and dynamic binding options. ("What is Python? | python.org")

Its toolset makes it a modular and agile language, suitable for both rapid tactical tasks and longer-range strategic application development efforts. In fields such as Internet scripting, systems programming, user interfaces, product customization, numeric programming, and more, Python is used by at least hundreds of thousands of developers around the world.(Lutz, 2017)

Description of the Software

The software is mainly designed to analyze the characteristic parameters of seismic isolation systems of buildings and prepare their reports. It helps us to analyze the behavior of the structures by defining the changes between the maximum and minimum values on the parameter that the user wants to analyze. This allows us to save time, as it quickly affects the changes and reports on the structure.

The software uses the Python programming language base and libraries. Libraries are generally math and graphic libraries. Prepared for the UBC-97 regulation. It can be seen flowchart of calculation routine in Figure 3.

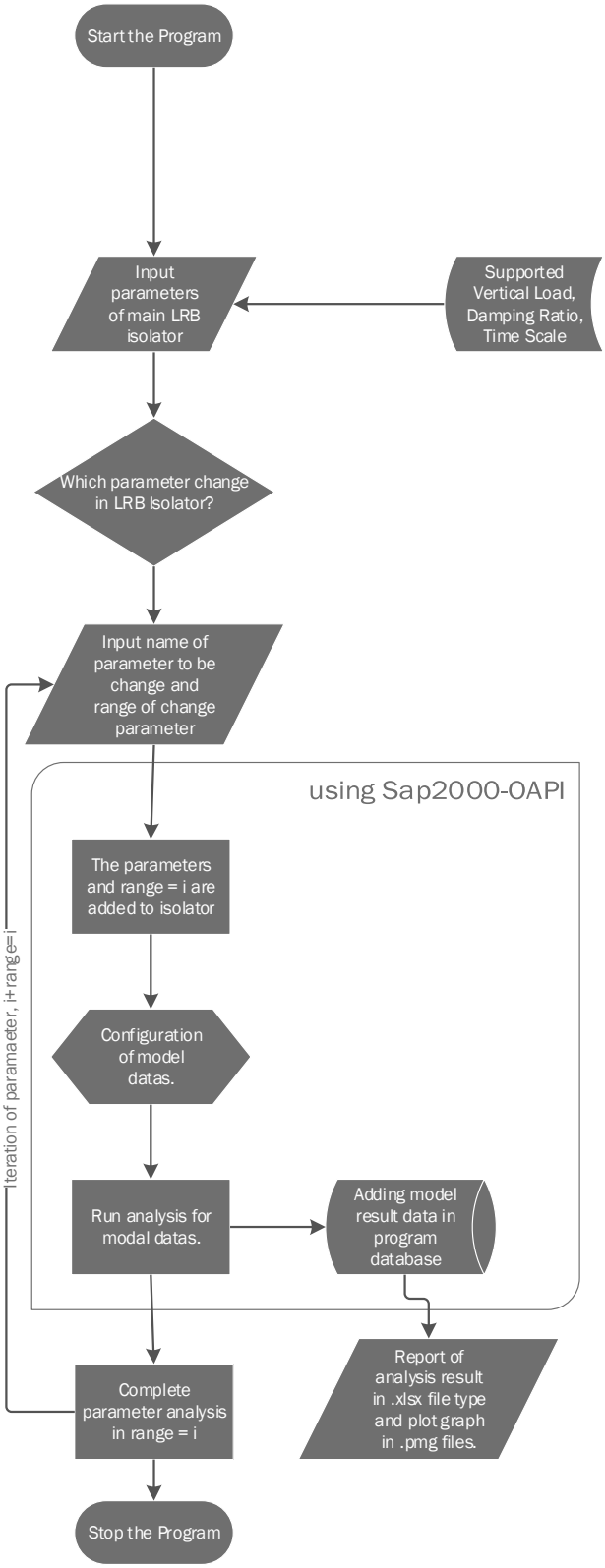

Figure 3: Software's flowchart.

Pseudocode for Parameter Iteration Module

```
import python library for manage data, plotting and SAP2000 OAPI module

input("please type for parameter of main lrb isolator", vertical load,
damping, time scale)

calculation for isolator parameters

selected_parameter = input("which parameter to be iterated", effective
stiffness, effective damping, yield strength etc.)

for seleceted_parameter in range(i, min, max)

        set calculated isolator parameters to example structure model

        define and configuration loads

        run analysis

        get results of example structure model

        found base isolator displacement in SAP2000 analysis results

        result datas exporting to .xlxs file and plotting chart and
diagram                                                    to .png file

        i += 1

print("Done!")
```

Non-Software Seismic Isolator Design According to UBC-97

According to UBC-97, the design of the lead core rubber isolator for the structure with the following characteristics is explained in this section with numerical application.

Table 12: SUBJECT STRUCTURE FEATURES

Number of Floors	**5**
Total Building Height, (H)	17,5 (m)
Floor Height	3,5 (m)
Column Dimensions	50x50 (cm)
Beam Dimensions	25x50 (cm)
Material Information	
Concrete	C35 (fcm = 35 Mpa)
Reinforcing Steel	S420 (fyk = 240 Mpa)

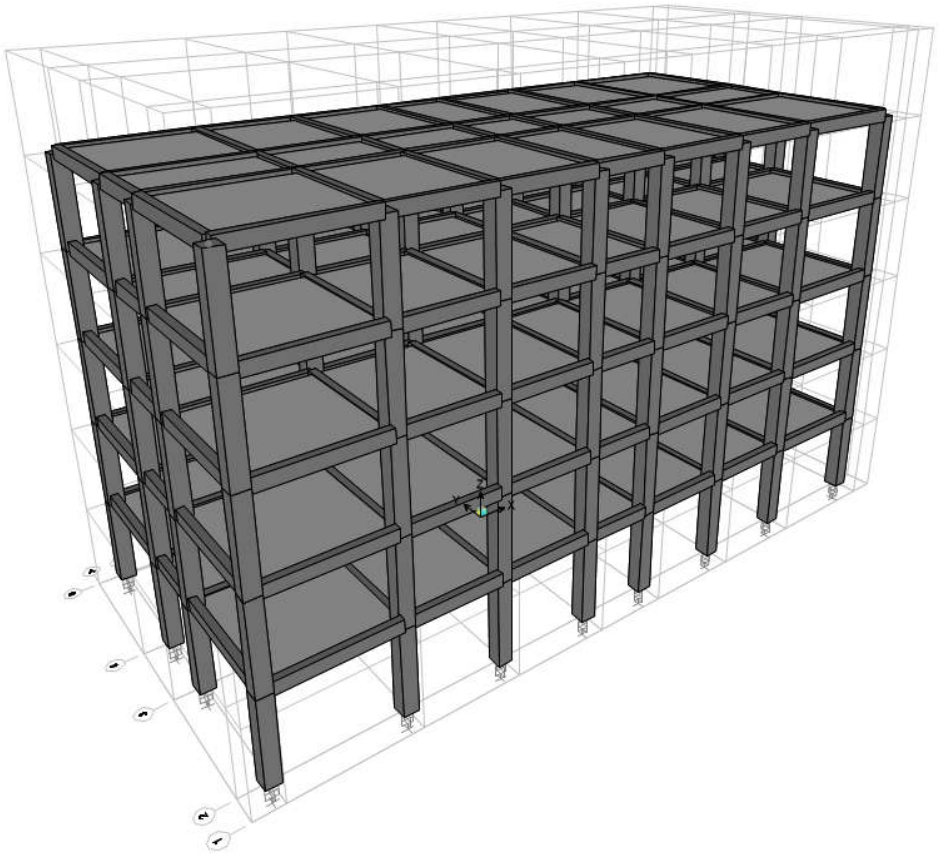

Figure 4: Three-dimensional view of the subject building.

Table 13: SEISMIC PROPERTIES OF THE SUBJECT STRUCTURE ACCORDING TO UBC-97

Seismic Source Type	**A**	**(UBC 97 Table 16-U)**
Distance to Known Source Fault (km)	5 km	**(UBC 97 Table 16-I)**
Seismic Zone Coefficient, (Z)	0.4	**(UBC 97 Table 16-I)**
Soil Profile Type	Sc	**(UBC 97 Table 16-J)**
Near Fault Coefficient, (NA)	1.2	**(UBC 97 Table 16-S)**
Near Fault Coefficient, (NV)	1.6	**(UBC 97 Table 16-T)**
Seismic Coefficient, (CA)	0.4	**(UBC 97 Table 16-Q)**
Seismic Coefficient, (CV)	0.56	**(UBC 97 Table 16-R)**
MCE Behavior Coefficient, (MM)	1.25	**(UBC 97 Table A-16-D)**
Seismic Coefficient, (CAM)	0.66	**(UBC 97 Table A-16-F)**
Seismic Coefficient, (CVM)	0.88	**(UBC 97 Table A-16-G)**

Numerical Application:

Normal forces acting on the columns (50x50 cm): 2303 kN

Natural vibration period of the structure: 0.81 s

$$T_D \geq 3 \times T_{ENCASTRE} = 3 \times 0.81 = 2.43 \quad \textbf{(Eq. 29)}$$

$$T_D = 2.5\ s\ selected$$

Isolator Design

- *Calculation of effective horizontal stiffness*

$$d_D = (g \times C_{VD} \times T_D)/(B_D \times 4\pi^2) = (9.81 \times 0.48 \times 2.5)/(1.2 \times 4\pi^2) = 0.248\ (Percentage\ of\ damping\ 10\%) \quad \textbf{(Eq. 30)}$$

$$d_M = (g \times C_{VM} \times T_M)/(B_D \times 4\pi^2) = (9.81 \times 0.89 \times 3)/(1.2 \times 4\pi^2) = 0.46\ (Percentage\ of\ damping\ 10\%) \quad \textbf{(Eq. 31)}$$

- *Calculation of design and maximum displacements*

$$K_H = K_{eff} = (w/g) \times (2\pi/T_D)^2 = (2303/9.81) \times (2\pi/2.5)^2 = 1482.87 kN/m \quad \textbf{(Eq. 32)}$$

$$W_D = 2\pi \times K_{eff} \times (d_D)^2 \times \beta_{eff} = 2\pi \times 1482.87 \times (0.248)^2 \times 0.1 = 57.304\ kNm \quad \textbf{(Eq. 33)}$$

- *Calculation of characteristic strength*

$$W_D = 4 \times Q_d \times (d_D - d_Y) \quad \textbf{(Eq. 34)}$$

$$Q_D = W_D/(4 \times d_D) = 57.304/(4 \times 0.248) = 57.766 \quad \textbf{(Eq. 35)}$$

- *Calculation of yield displacement*

$$d_y = Q_D/(K_u \times K_d) \quad \textbf{(Eq. 36)}$$

$$K_u = 10 \times K_d \quad \textbf{(Eq. 37)}$$

$$K_d = K_{eff} - (Q_d/d_d) = 1482.87 - (57.766/0.248) = 1249.94kN \quad \textbf{(Eq. 38)}$$

$$d_y = Q_d/(9 \times K_d) = 57.766/(9 \times 1249.94) = 0.005135m \quad \textbf{(Eq. 39)}$$

- *Calculation of lead core cross-section*

$$A_{pb} = Q_d/f_y = 57.766/11 = 5251mm^2 \quad \textbf{(Eq. 40)}$$

If lead core diameter is selected as 45 mm, lead core cross-section area will be 6361 mm^2.

$$(6361 > 5251)$$

In this case, the Q_d value is recalculated for the cross section area of 6361 mm^2.

$$Q_d = 6361 \times 11 = 69.97kN \quad \textbf{(Eq. 41)}$$

- *Calculation of the stiffness provided by the lead core*

$$K_{pb} = Q_d/d_D = 69.97/0.248 = 282.137mm^2 \quad \textbf{(Eq. 42)}$$

- *Calculation of the stiffness provided by the rubber part*

$$K_{rub} = K_d = K_H - K_{pb} = 1482.87 - 282.137 = 1200.733kN/m \quad \textbf{(Eq. 43)}$$

- *Calculation of the cross-section of the rubber part*

$$A_{rub} = (\pi \times 500^2)/4 - 6361 = 189988mm^2 \quad \textbf{(Eq. 44)}$$

- *Calculation of the required total rubber thickness*

$$t_r = (G \times A_{rub})/K_{rub} = (0.5 \times 189988)/1200.733 = 79.11mm \quad \textbf{(Eq. 45)}$$

- *Calculation of the shape factor*

$$S = \theta/(4 \times t) = 0.5/(4 \times 0.005)\ (thickness\ of\ a\ single\ rubber\ layer\ 5mm) = 25 \quad \textbf{(Eq. 46)}$$

- *Calculation of the vertical stiffness of the isolator*

$$K_v = (E_c \times A_s)/t_r = (6 \times G \times S^2)/t_r = (6 \times 0.5 \times 25^2 \times 196349)/79.11 = 4653702kN/m \quad \textbf{(Eq.47)}$$

- *Calculation of the required total rubber thickness*

$$F_y = Q_d + K_d \times d_y = 69.97 + 1249.94 \times 0.005135 = 76.38kN \quad \textbf{(Eq. 48)}$$

- *Determination of total isolator height*

The required total rubber thickness was calculated as 79.11 mm. A single rubber layer thickness was chosen as 5 mm. Required rubber layer thickness can be provided with a total of 16 rubber layers. Between these 16 layers, there will be 15 pieces of 3 mm thick steel plates. By selecting the upper and lower steel plate thickness 30 mm, the total isolator height can be calculated as follows.

$$h_{total} = 16 \times 5 + 15 \times 3 + 2 \times 30 = 185mm \quad \textbf{(Eq. 49)}$$

- *Calculation of slip shape deformations*

For vertical;

$$\Delta_t = W/k_v = 2303/4653702 = 0.494mm \quad \textbf{(Eq. 50)}$$

$$\varepsilon_z = \Delta t/h_{top} = 0.494/185 = 0.00267 \quad \textbf{(Eq. 51)}$$

$$y_v = 6 \times S \times \varepsilon_z = 6 \times 25 \times 0.00267 = 0.4 \quad \textbf{(Eq. 52)}$$

- *Calculation of slip shape deformations*

For horizontal;

$$y_s = \tau/G = V_D/(A_s \times G) = (K_d \times d_d)/(A_s \times G) = (1249940 \times 0.248)/(0.196 \times 0.5 \times 10^6) = 3.16 \quad \textbf{(Eq. 53)}$$

The maximum deformation is;

$$y_{max} = y_v \times y_s = 0.4 + 3.16 = 3.2 \quad \textbf{(Eq. 54)}$$

- *Common area calculations*

$$sin\theta = d_D/D = 0.248/0.5 = 0.496 \quad \textbf{(Eq. 55)}$$

$$\theta = 29.7357^{\circ} = 0.5189rad \quad \textbf{(Eq. 56)}$$

$$\cos(\theta) = 0.8683 \quad \textbf{(Eq. 57)}$$

$$A' = A_s[1 - 2/\pi(\theta + sin\theta \times cos\theta)] = 0.196[1 - 2/\pi(0.5189 + 0.496 \times 0.8683)] = 0.07751m^2 \quad \textbf{(Eq. 58)}$$

- *Calculation of critical buckling load*

The load that a single isolator can carry without causing buckling is calculated by the formula below.

$$P_{critical} = \sqrt{((A \times G \times \pi^2 \times E_c \times I)/(3t^2))} \quad \textbf{(Eq. 59)}$$

$$I = (\pi/4) \times (\theta/2)^4 \quad \textbf{(Eq. 60)}$$

$$P_{critical} = \sqrt{((0.196 \times 0.5 \times 10^3 \times \pi^2 \times 1200 \times 10^3 \times 0.25^4 \times 0.25)/(3 \times 0.185^2))} = 3322.54kN \quad \textbf{(Eq. 61)}$$

With the designed analysis software, the isolator parameters of the sample structure, the numerical sample of which is made, are specified in the previous topic. The effect of changes of these parameters on the structure will be examined in this section. It is also given in this section which parameters change in what range.

The main isolator parameters used in the building are specified in the table.

Table 14: ISOLATOR PARAMETERS TO BE USED IN THE SUBJECT STRUCTURE

U1 – Effective stiffness (kN/m)	4653702
U2 – Effective stiffness (kN/m)	1482.87
U2 – Yield Strength (kN)	76.38
U2 – Post Yield Stiffness Ratio (K_d/K_u)	0.1
U3 – Effective stiffness (kN/m)	1482.87
U3 – Yield Strength (kN)	76.38
U3 – Post Yield Stiffness Ratio (K_d/K_u)	0.1

Parameter Iteration Module – Monitoring the Increment of the Calculated K_V Parameter in Lead Rubber Bearing Type Isolator Model

The initial value for K_V, one of the isolator parameters, was determined as 4653702 kN/m in the calculations. The limit of the iteration is considered as 10000000 and the increment value as 1000000.

Table 15: EFFECTIVE STIFFNESS (U1) – INCREMENT VALUES FOR K_V PARAMETER

Parameter	Effective Stiffness (U1) – K_v
First Step	4653702 kN/m
Last Step	9653702 kN/m
Number of Steps	6
Step Range	1000000 kN/m

The first step is for K_V = 4653702 kN/m;

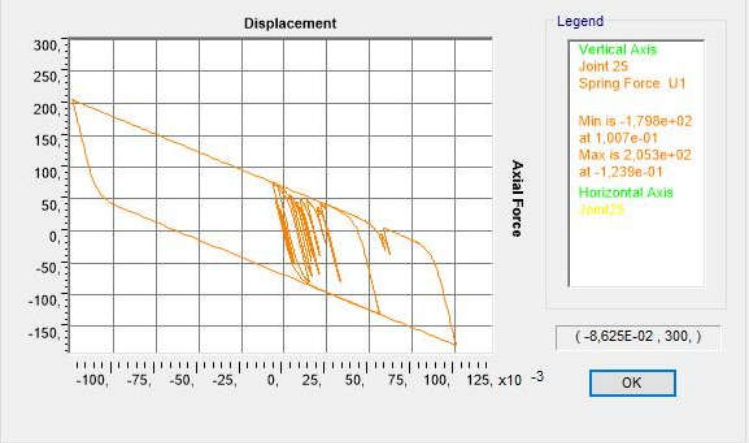

Figure 5: Lead Rubber Bearing's hysteresis loop for K_V = 4653702 kN/m.

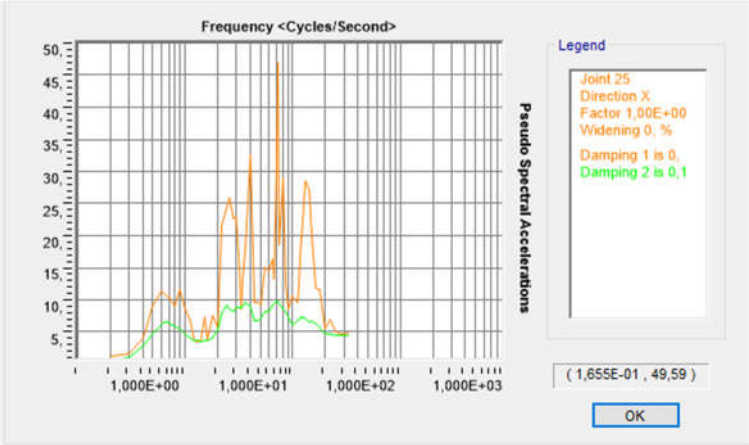

Figure 6: Response spectrum curves for K_V = 4653702 kN/m.

Table 16: COORDINATES AND DISPLACEMENTS OF POINTS ON 3-G AXIS FOR K_V = 4653702 KN/M

Point Number	U1 Coordinates (m)	U2 Coordinates (m)	U3 Coordinates (m)	U1 Displacement (m)	U2 Displacement (m)	U3 Displacement (m)
127	6.1	-2.65	0	4.67132E-07	-0.016003299	-1.65632E-05
128	6.1	-2.65	3.5	5.88091E-12	-0.019687365	-3.8604E-05
129	6.1	-2.65	7	6.56824E-12	-0.022297903	-5.22124E-05
130	6.1	-2.65	10.5	6.91067E-12	-0.024099921	-5.91499E-05
131	6.1	-2.65	14	7.31161E-12	-0.025307785	-6.2137E-05
132	6.1	-2.65	17.5	7.47442E-12	-0.026034541	-6.28848E-05

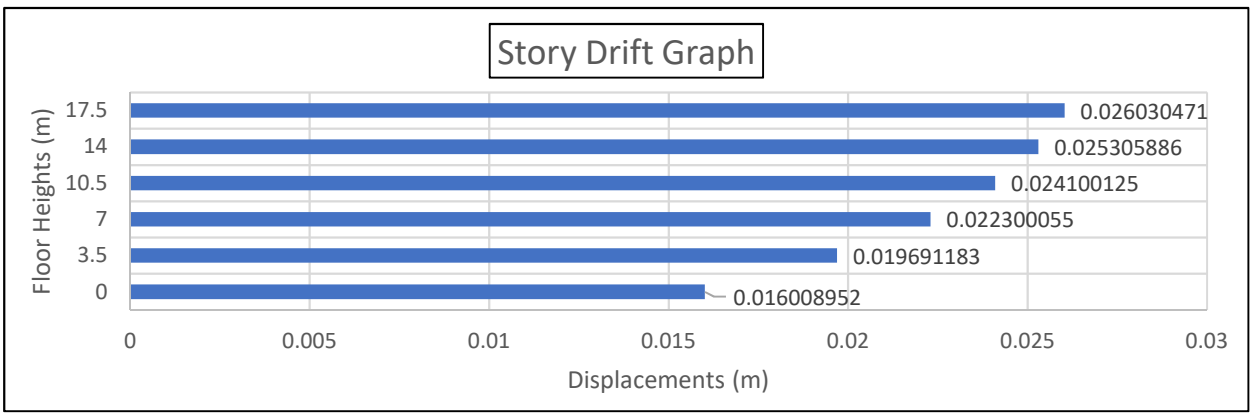

Figure 7: Story Drift Graph of Points On 3-G Axis for K_V = 4653702 kN/m

The second step is for, K_V = 5653702 kN/m;

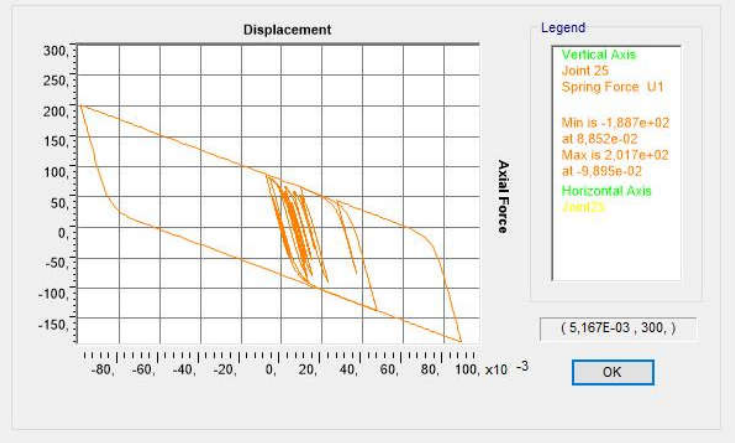

Figure 8: Lead Rubber Bearing's hysteresis loop for K_V = 5653702 kN/m.

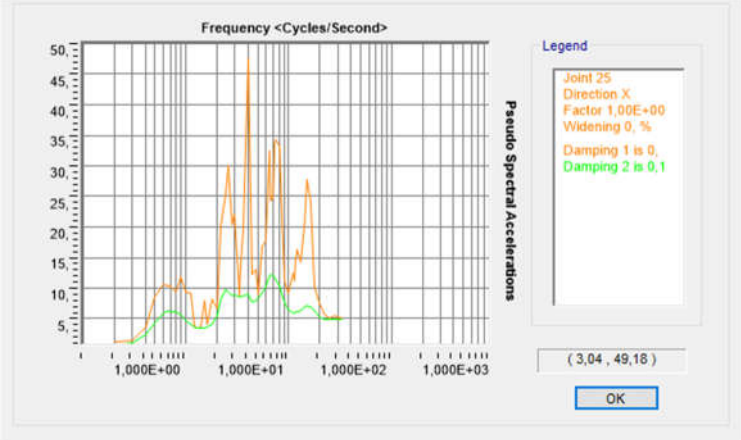

Figure 9: Response spectrum curves for K_V = 5653702 kN/m.

Table 17: COORDINATES AND DISPLACEMENTS OF POINTS ON 3-G AXIS FOR K_V = 5653702 KN/M

Point Number	U1 Coordinates (m)	U2 Coordinates (m)	U3 Coordinates (m)	U1 Displacement (m)	U2 Displacement (m)	U3 Displacement (m)
127	6.1	-2.65	0	-4.70746E-07	0.016008952	1.37271E-05
128	6.1	-2.65	3.5	-5.87331E-12	0.019691183	3.5919E-05
129	6.1	-2.65	7	-6.55927E-12	0.022300055	4.96456E-05
130	6.1	-2.65	10.5	-6.90143E-12	0.024100125	5.66685E-05
131	6.1	-2.65	14	-7.30217E-12	0.025305886	5.97111E-05
132	6.1	-2.65	17.5	-7.46393E-12	0.026030471	6.04851E-05

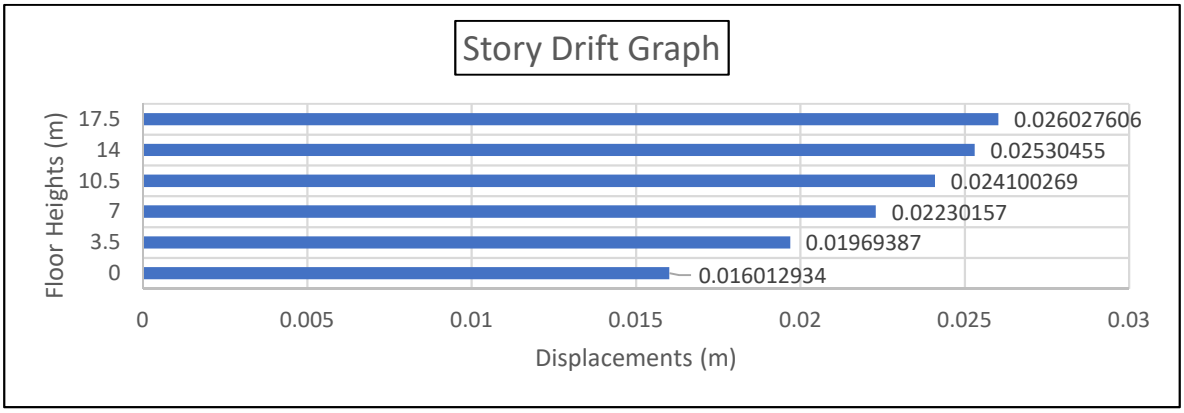

Figure 10: Story Drift Graph of Points On 3-G Axis for K_V = 5653702 kN/m

The third step is for K_V = 6653702 kN/m;

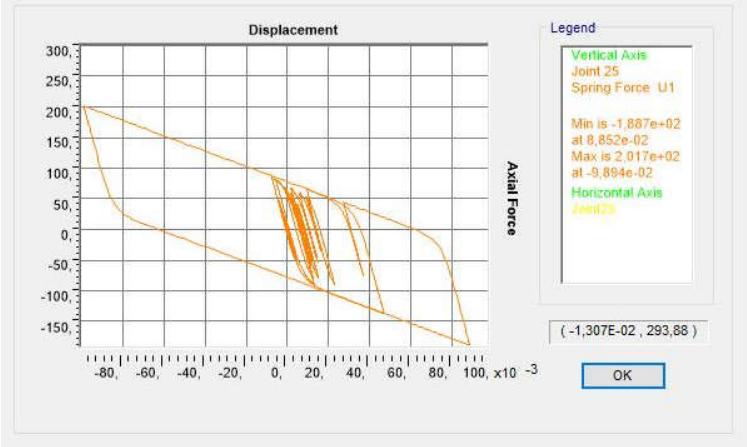

Figure 11: Lead Rubber Bearing's hysteresis loop for K_V = 6653702 kN/m.

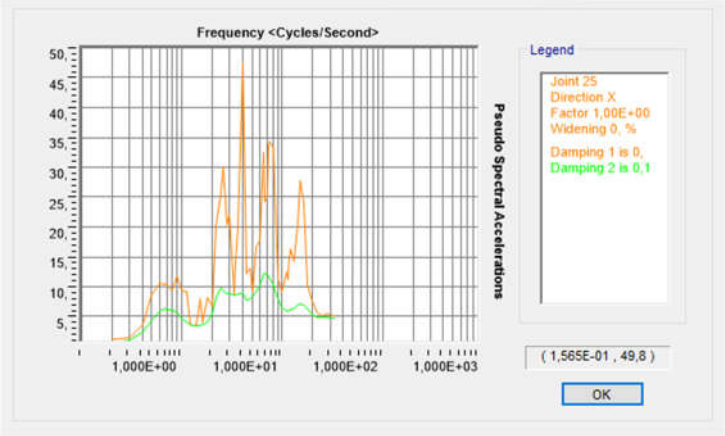

Figure 12: Response spectrum curves for K_V = 6653702 kN/m.

Table 18: **COORDINATES AND DISPLACEMENTS OF POINTS ON 3-G AXIS FOR K_V = 6653702 KN/M**

Point Number	U1 Coordinates (m)	U2 Coordinates (m)	U3 Coordinates (m)	U1 Displacement (m)	U2 Displacement (m)	U3 Displacement (m)
127	6.1	-2.65	0	4.7347E-07	0.016012934	-1.17203E-05
128	6.1	-2.65	3.5	5.87479E-12	0.01969387	-3.40195E-05
129	6.1	-2.65	7	6.5609E-12	0.02230157	-4.783E-05
130	6.1	-2.65	10.5	6.90376E-12	0.024100269	-5.49135E-05
131	6.1	-2.65	14	7.30489E-12	0.02530455	-5.79954E-05
132	6.1	-2.65	17.5	7.46622E-12	0.026027606	-5.87881E-05

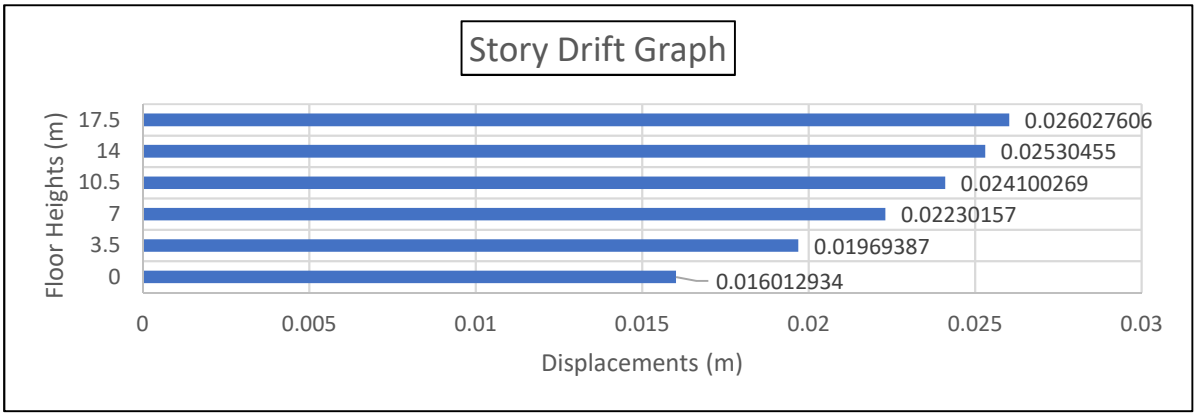

Figure 13: Story Drift Graph of Points On 3-G Axis for K_V = 6653702 kN/m

The fourth is for K_V = 7653702 kN/m;

Figure 14: Lead Rubber Bearing's hysteresis loop for K_V = 7653702 kN/m.

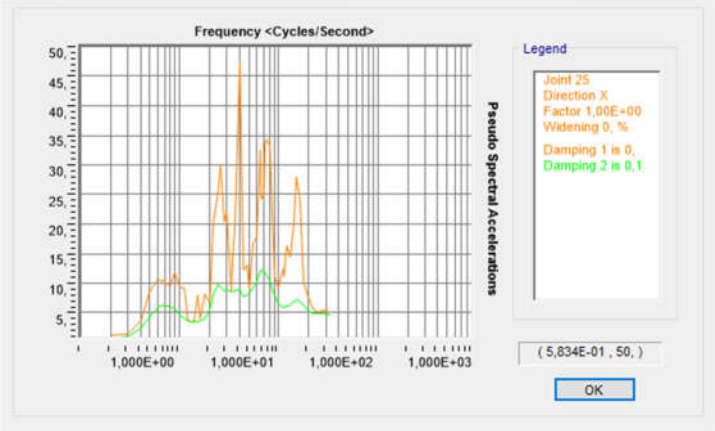

Figure 15: Response spectrum curves for K_V = 7653702 kN/m.

Table 19: COORDINATES AND DISPLACEMENTS OF POINTS ON 3-G AXIS FOR K_V = 7653702 KN/M

Point Number	U1 Coordinates (m)	U2 Coordinates (m)	U3 Coordinates (m)	U1 Displacement (m)	U2 Displacement (m)	U3 Displacement (m)
127	6.1	-2.65	0	-4.75589E-07	0.01601589	1.02256E-05
128	6.1	-2.65	3.5	-5.897E-12	0.019695863	3.26047E-05
129	6.1	-2.65	7	-6.58556E-12	0.022302693	4.64778E-05
130	6.1	-2.65	10.5	-6.93025E-12	0.024100375	5.36066E-05
131	6.1	-2.65	14	-7.33253E-12	0.025303558	5.67179E-05
132	6.1	-2.65	17.5	-7.49408E-12	0.02602548	5.75245E-05

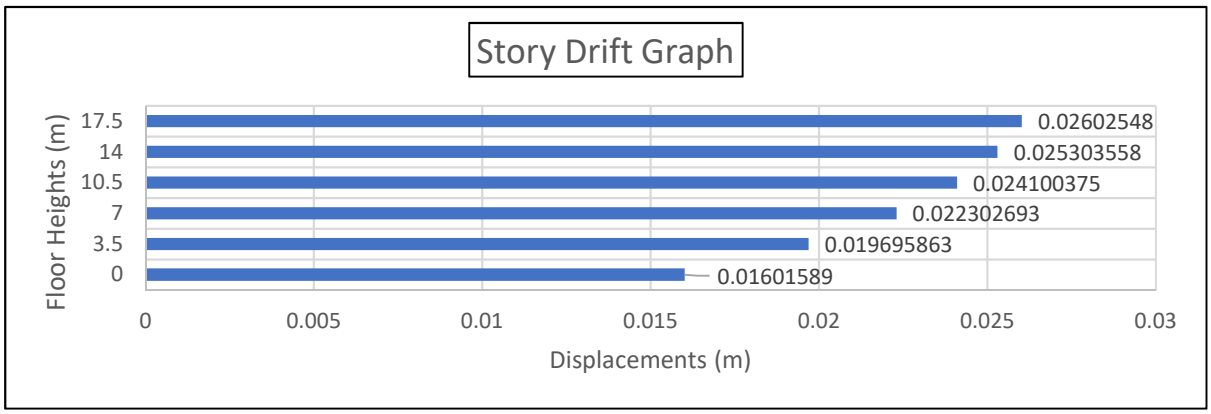

Figure 16: Story Drift Graph of Points On 3-G Axis for K_V = 7653702 kN/m

The fifth step is for K_V = 8653702 kN/m;

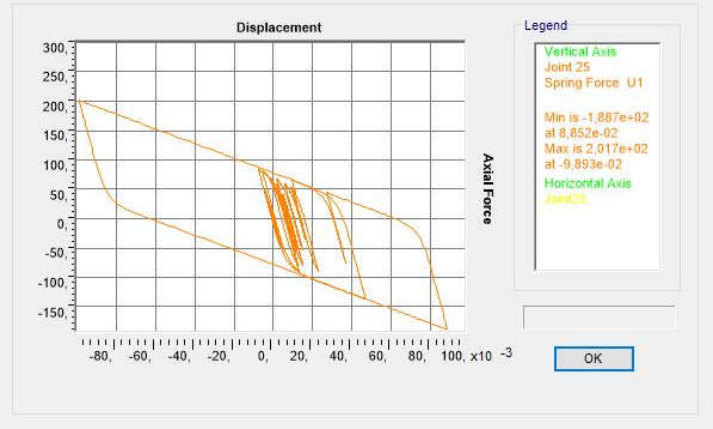

Figure 17: Lead Rubber Bearing's hysteresis loop for K_V = 8653702 kN/m.

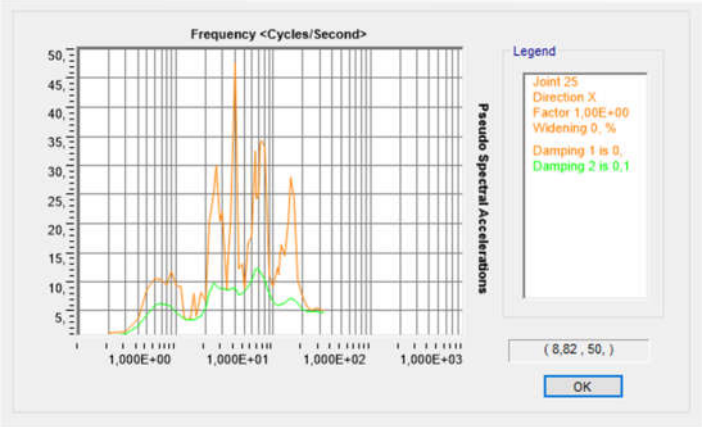

Figure 18: Response spectrum curves for K_V = 8653702 kN/m.

Table 20: COORDINATES AND DISPLACEMENTS OF POINTS ON 3-G AXIS FOR K_V = 8653702 KN/M

Point Number	U1 Coordinates (m)	U2 Coordinates (m)	U3 Coordinates (m)	U1 Displacement (m)	U2 Displacement (m)	U3 Displacement (m)
127	6.1	-2.65	0	-4.77283E-07	0.016018171	9.06897E-06
128	6.1	-2.65	3.5	-5.99398E-12	0.019697401	3.15101E-05
129	6.1	-2.65	7	-6.69363E-12	0.02230356	4.54317E-05
130	6.1	-2.65	10.5	-7.04565E-12	0.024100456	5.25956E-05
131	6.1	-2.65	14	-7.45268E-12	0.025302792	5.57297E-05
132	6.1	-2.65	17.5	-7.61668E-12	0.02602384	5.65471E-05

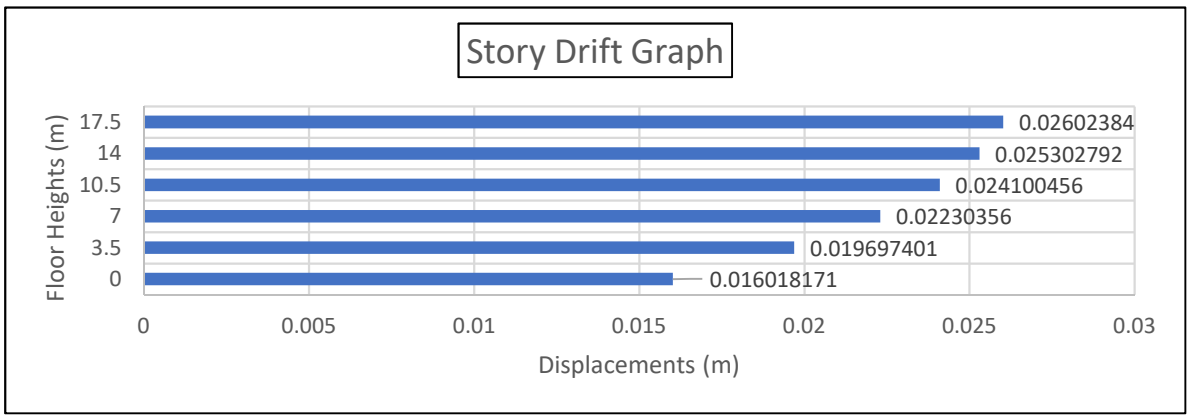

Figure 19: Story Drift Graph of Points On 3-G Axis for K_V = 8653702 kN/m.

The sixth step is for K_V = 9653702 kN/m;

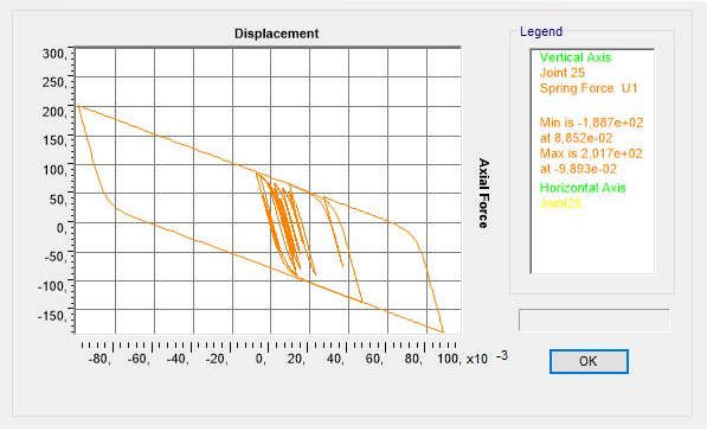

Figure 20: Lead Rubber Bearing's hysteresis loop for K_V = 9653702 kN/m.

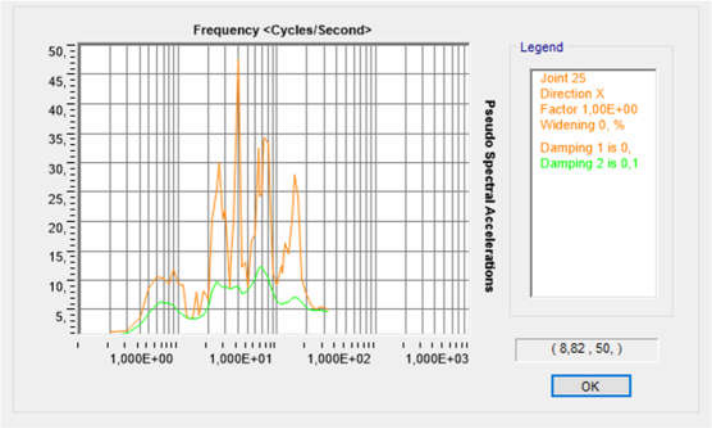

Figure 21: Response spectrum curves for K_V = 9653702 kN/m.

Table 21: COORDINATES AND DISPLACEMENTS OF POINTS ON 3-G AXIS FOR K_V = 9653702 KN/M

Point Number	U1 Coordinates (m)	U2 Coordinates (m)	U3 Coordinates (m)	U1 Displacement (m)	U2 Displacement (m)	U3 Displacement (m)
127	6.1	-2.65	0	4.78666E-07	0.016019985	-8.14746E-06
128	6.1	-2.65	3.5	5.91248E-12	0.019698624	-3.06381E-05
129	6.1	-2.65	7	6.6021E-12	0.022304249	-4.45984E-05
130	6.1	-2.65	10.5	6.94803E-12	0.024100521	-5.17902E-05
131	6.1	-2.65	14	7.3512E-12	0.025302183	-5.49424E-05
132	6.1	-2.65	17.5	7.5127E-12	0.026022536	-5.57685E-05

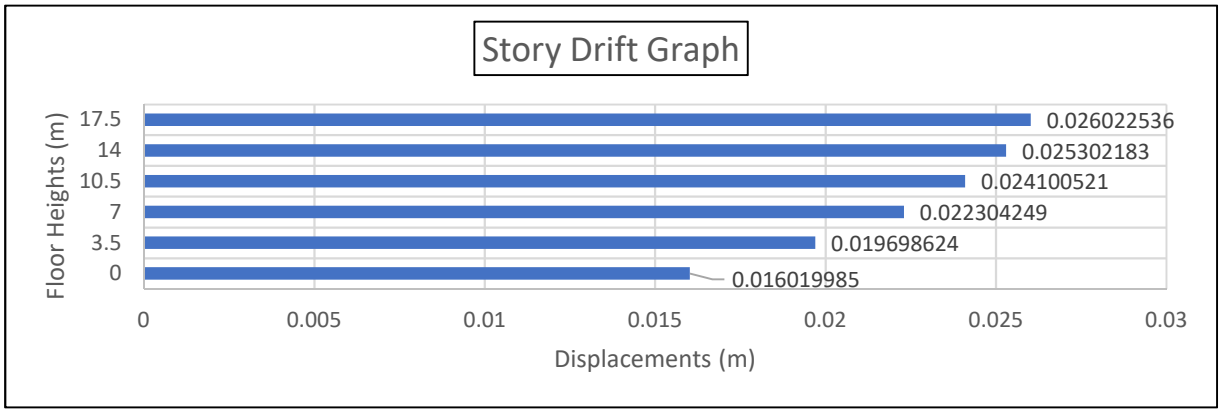

Figure 22: Story Drift Graph of Points On 3-G Axis for K_V = 9653702 kN/m

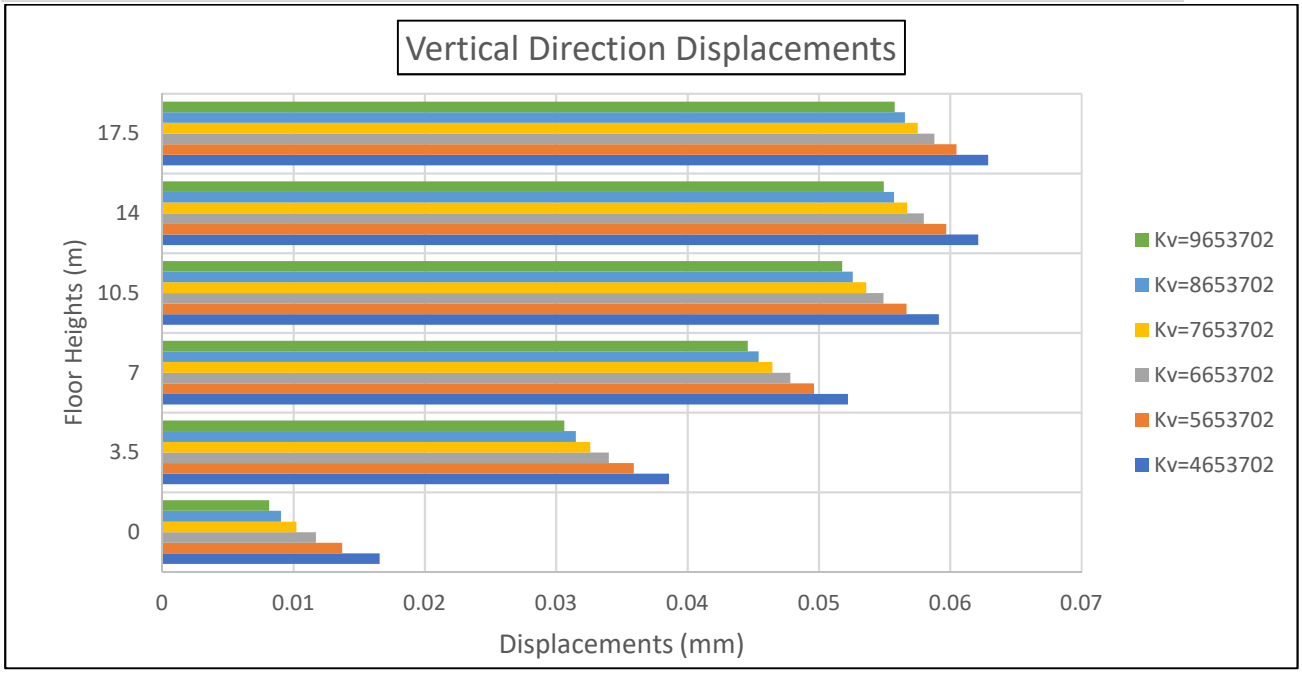

Figure 23: Effect of parameter, effective stiffness on vertical displacement of the structure.

Parameter Iteration Module – Monitoring the Increment of the Calculated F_y Parameter in Lead Rubber Bearing Type Isolator Model

The initial value for yield strength, one of the isolator parameters, was determined as 76.38 kN in the calculations. The limit of the iteration is considered as 200 kN and the increment value as 20.

Table 22: YIELD STRENGTH – INCREMENT VALUES FOR F_Y PARAMETER

Parameter	Yield Strength – F_y
First Step	76.38 kN
Last Step	196.38 kN/m
Number of Steps	7
Step Range	20 kN

The first step is for F_y= 76.38 kN;

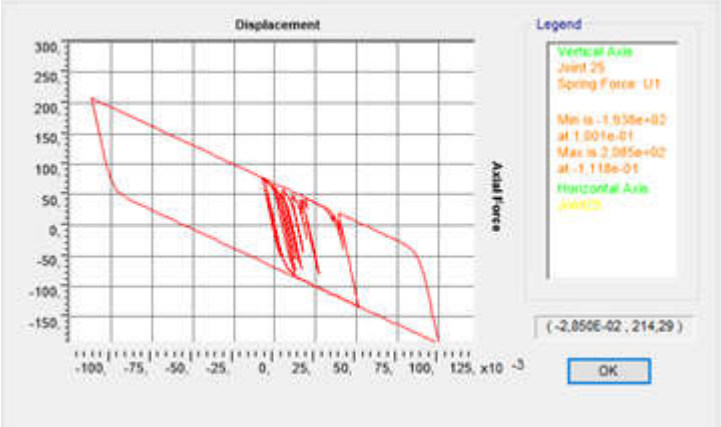

Figure 24: Lead Rubber Bearing's hysteresis loop for F_y= 76.38 kN.

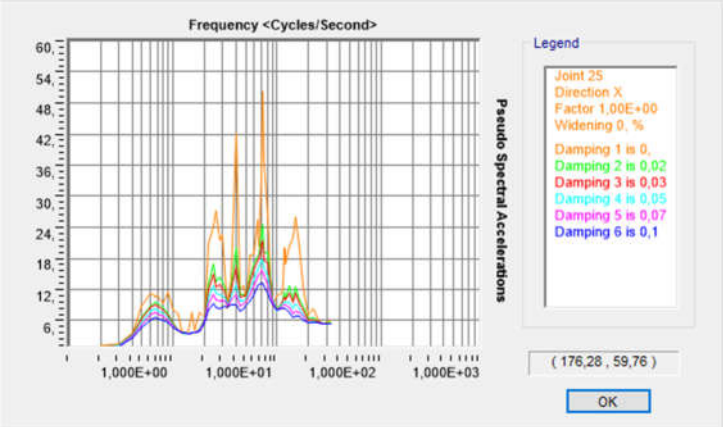

Figure 25: Response spectrum curves for F_y = 76.38 kN.

Table 23: COORDINATES AND DISPLACEMENTS OF POINTS ON 3-G AXIS FOR F_y= 76.38 KN.

Point Number	U1 Coordinates (m)	U2 Coordinates (m)	U3 Coordinates (m)	U1 Displacement (m)	U2 Displacement (m)	U3 Displacement (m)
127	6.1	-2.65	0	4.67134E-07	0.016003299	-1.65632E-05
128	6.1	-2.65	3.5	7.21955E-12	0.019687365	-3.8604E-05
129	6.1	-2.65	7	8.07834E-12	0.022297903	-5.22124E-05
130	6.1	-2.65	10.5	8.65341E-12	0.024099921	-5.91499E-05
131	6.1	-2.65	14	9.04929E-12	0.025307785	-6.2137E-05
132	6.1	-2.65	17.5	9.25182E-12	0.026034541	-6.28848E-05

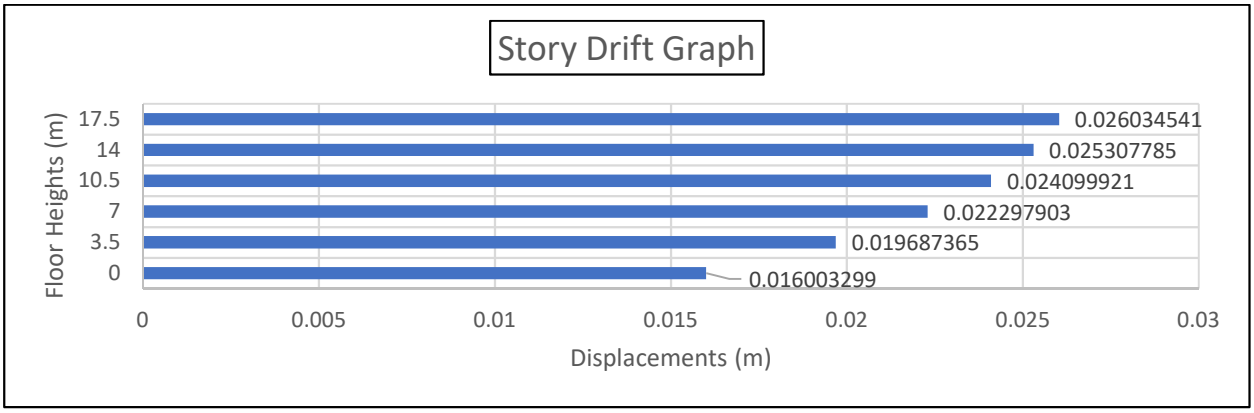

Figure 26: Story Drift Graph of Points on 3-G Axis for F_y = 76.38 kN.

The second step is for F_y = 96.38 kN;

Figure 27: Lead Rubber Bearing's hysteresis loop for F_y = 96.38 kN.

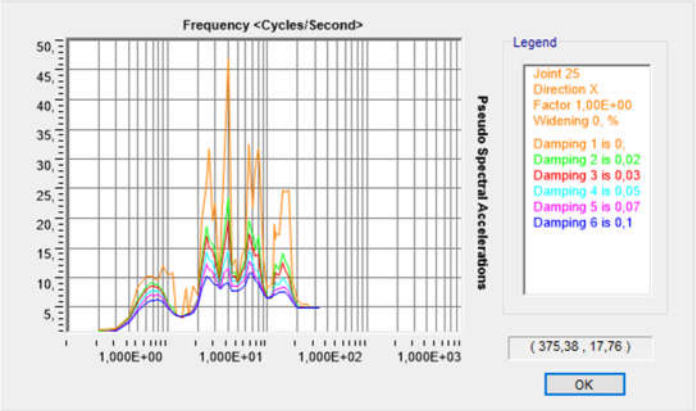

Figure 28*:* Response spectrum curves for F_y = 96.38 kN.

Table 24: COORDINATES AND DISPLACEMENTS OF POINTS ON 3-G AXIS FOR F_y = 96.38 KN.

Point Number	U1 Coordinates (m)	U2 Coordinates (m)	U3 Coordinates (m)	U1 Displacement (m)	U2 Displacement (m)	U3 Displacement (m)
127	6.1	-2.65	0	4.67134E-07	0.016003299	-1.65632E-05
128	6.1	-2.65	3.5	7.21955E-12	0.019687365	-3.8604E-05
129	6.1	-2.65	7	8.07834E-12	0.022297903	-5.22124E-05
130	6.1	-2.65	10.5	8.65341E-12	0.024099921	-5.91499E-05
131	6.1	-2.65	14	9.04929E-12	0.025307785	-6.2137E-05
132	6.1	-2.65	17.5	9.25182E-12	0.026034541	-6.28848E-05

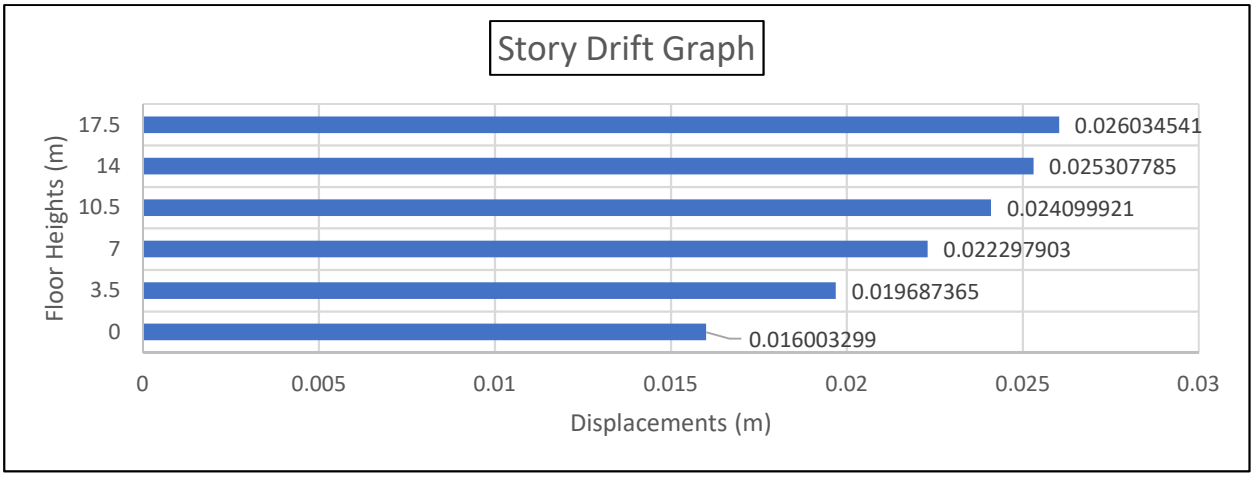

Figure 29: Story Drift Graph of Points on 3-G Axis for F_y = 96.38 kN.

The third step is for F_y = 116.38 kN;

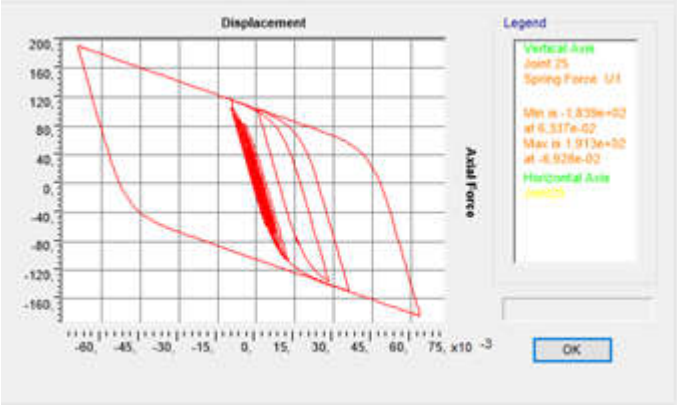

Figure 30: Lead Rubber Bearing's hysteresis loop for F_y = 116.38 kN.

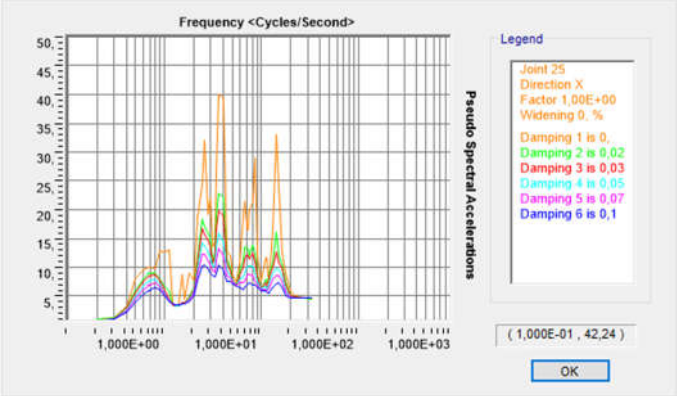

Figure 31: Response spectrum curves for F_y = 116.38 kN.

Table 25: COORDINATES AND DISPLACEMENTS OF POINTS ON 3-G AXIS FOR F_y = 116.38 KN.

Point Number	U1 Coordinates (m)	U2 Coordinates (m)	U3 Coordinates (m)	U1 Displacement (m)	U2 Displacement (m)	U3 Displacement (m)
127	6.1	-2.65	0	4.67134E-07	0.016003299	-1.65632E-05
128	6.1	-2.65	3.5	7.21955E-12	0.019687365	-3.8604E-05
129	6.1	-2.65	7	8.07834E-12	0.022297903	-5.22124E-05
130	6.1	-2.65	10.5	8.65341E-12	0.024099921	-5.91499E-05
131	6.1	-2.65	14	9.04929E-12	0.025307785	-6.2137E-05
132	6.1	-2.65	17.5	9.25182E-12	0.026034541	-6.28848E-05

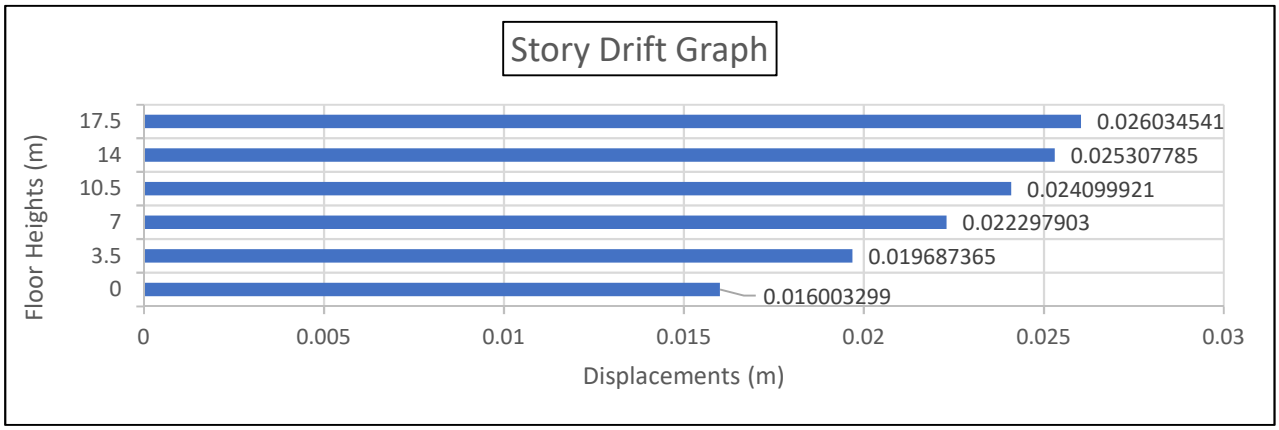

Figure 32: Story Drift Graph of Points On 3-G Axis for F_y = 116.38 kN.

The fourth step is for F_y = 136.38 kN;

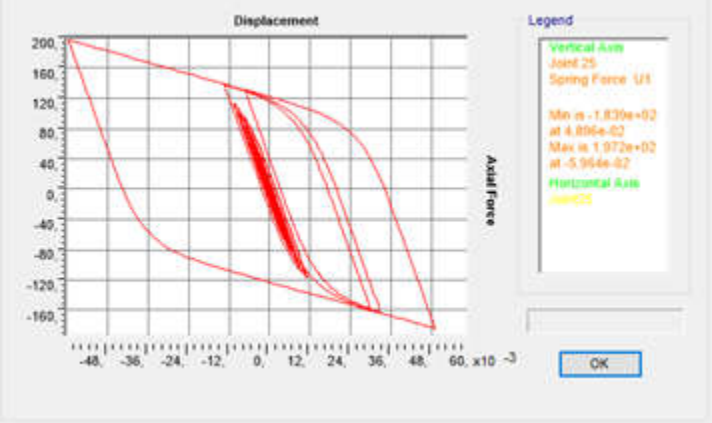

Figure 33: Lead Rubber Bearing's hysteresis loop for F_y = 136.38 kN.

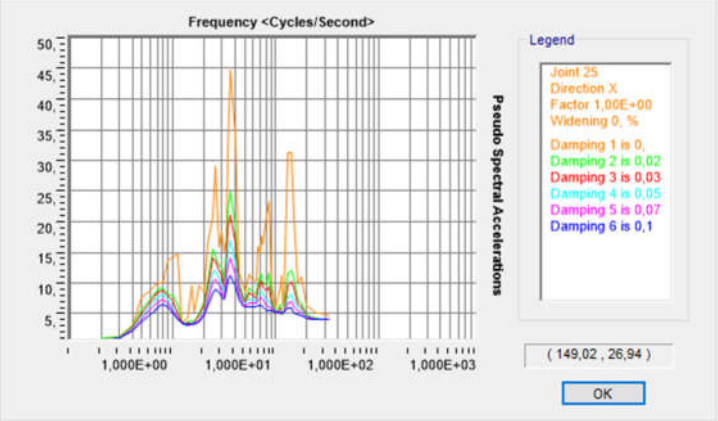

Figure 34: Response spectrum curves for F_y = 136.38 kN.

Table 26: COORDINATES AND DISPLACEMENTS OF POINTS ON 3-G AXIS FOR F_y = 136.38 KN.

Point Number	U1 Coordinates (m)	U2 Coordinates (m)	U3 Coordinates (m)	U1 Displacement (m)	U2 Displacement (m)	U3 Displacement (m)
127	6.1	-2.65	0	4.67134E-07	0.016003299	-1.65632E-05
128	6.1	-2.65	3.5	7.21955E-12	0.019687365	-3.8604E-05
129	6.1	-2.65	7	8.07834E-12	0.022297903	-5.22124E-05
130	6.1	-2.65	10.5	8.65341E-12	0.024099921	-5.91499E-05
131	6.1	-2.65	14	9.04929E-12	0.025307785	-6.2137E-05
132	6.1	-2.65	17.5	9.25182E-12	0.026034541	-6.28848E-05

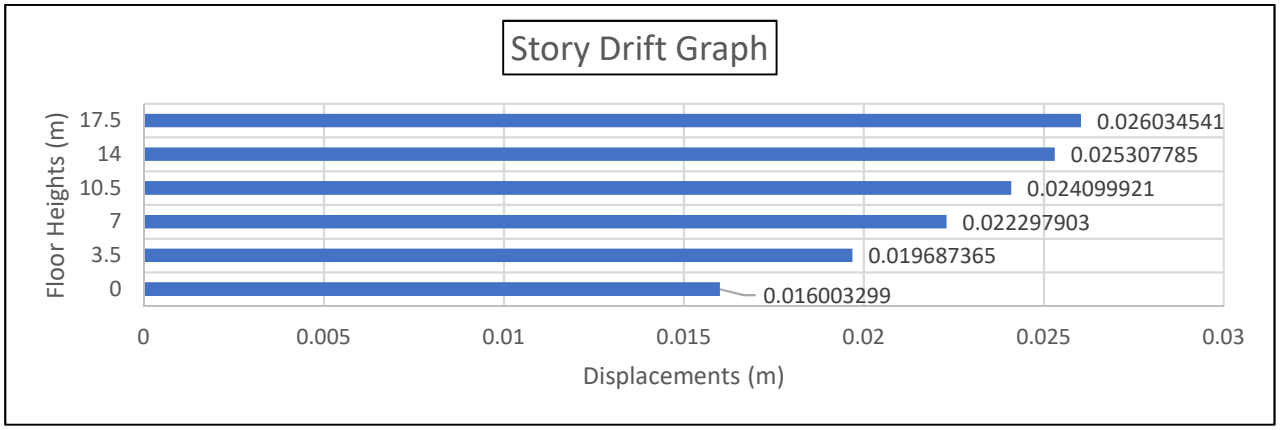

Figure 35: Story Drift Graph of Points On 3-G Axis for F_y = 136.38 kN.

The fifth step is for F_y = 156.38 kN;

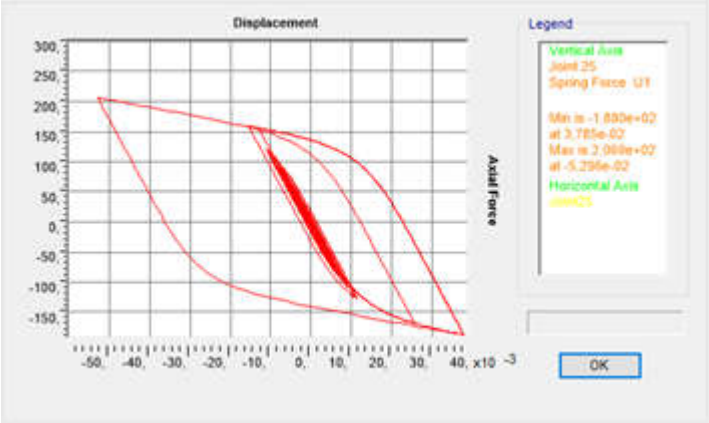

Figure 36: Lead Rubber Bearing's hysteresis loop for F_y = 156.38 kN.

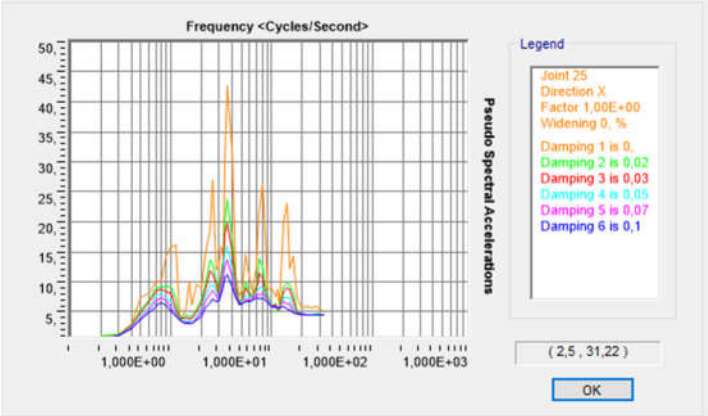

Figure 37: Response spectrum curves for F_y = 156.38 kN.

Table 27: COORDINATES AND DISPLACEMENTS OF POINTS ON 3-G AXIS FOR F_y = 156.38 KN.

Point Number	U1 Coordinates (m)	U2 Coordinates (m)	U3 Coordinates (m)	U1 Displacement (m)	U2 Displacement (m)	U3 Displacement (m)
127	6.1	-2.65	0	4.67134E-07	0.016003299	-1.65632E-05
128	6.1	-2.65	3.5	7.21955E-12	0.019687365	-3.8604E-05
129	6.1	-2.65	7	8.07834E-12	0.022297903	-5.22124E-05
130	6.1	-2.65	10.5	8.65341E-12	0.024099921	-5.91499E-05
131	6.1	-2.65	14	9.04929E-12	0.025307785	-6.2137E-05
132	6.1	-2.65	17.5	9.25182E-12	0.026034541	-6.28848E-05

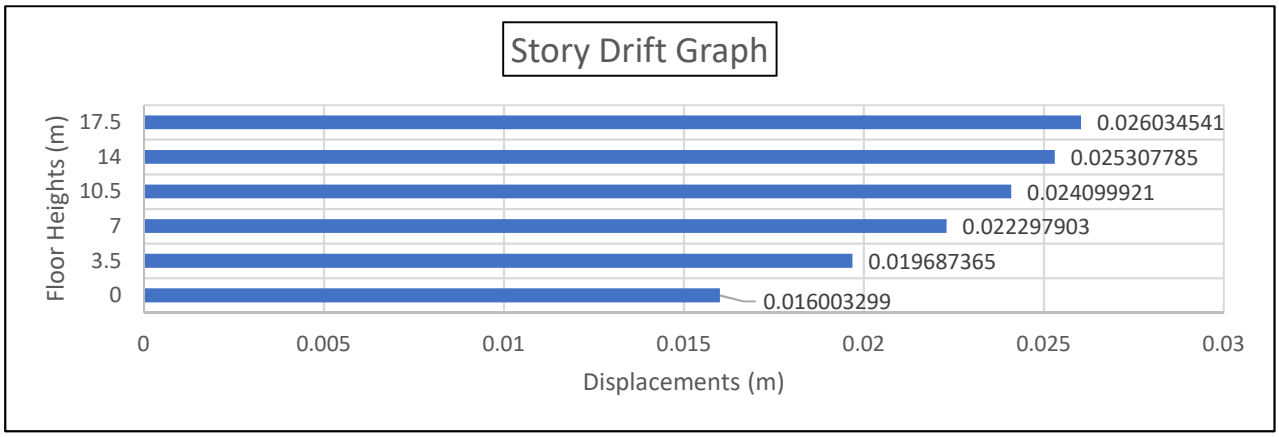

Figure 38: Story Drift Graph of Points on 3-G Axis for F_y = 156.38 kN.

The sixth step is for F_y = 176.38 kN;

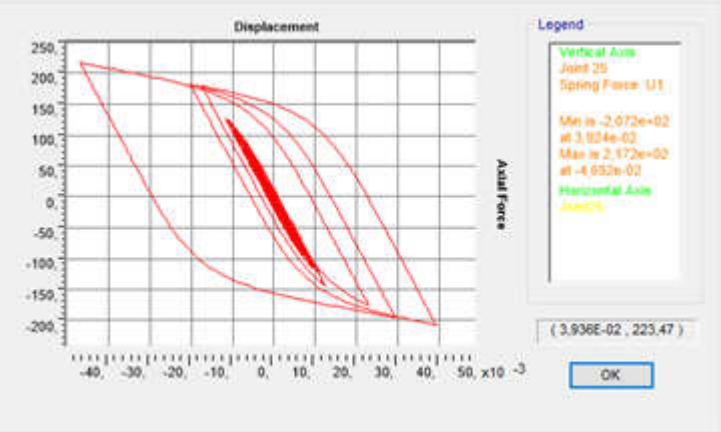

Figure 39: Lead Rubber Bearing's hysteresis loop for F_y = 176.38 kN.

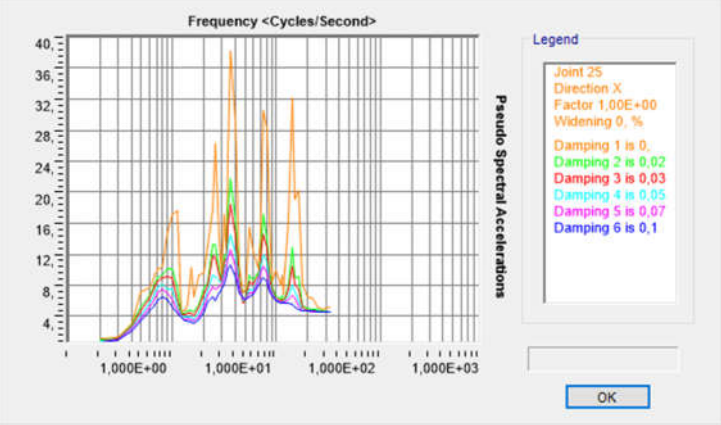

Figure 40: Response spectrum curves for F_y = 176.38 kN.

Table 28: COORDINATES AND DISPLACEMENTS OF POINTS ON 3-G AXIS FOR F_y = 176.38 KN.

Point Number	U1 Coordinates (m)	U2 Coordinates (m)	U3 Coordinates (m)	U1 Displacement (m)	U2 Displacement (m)	U3 Displacement (m)
127	6.1	-2.65	0	4.67134E-07	0.016003299	-1.65632E-05
128	6.1	-2.65	3.5	7.21955E-12	0.019687365	-3.8604E-05
129	6.1	-2.65	7	8.07834E-12	0.022297903	-5.22124E-05
130	6.1	-2.65	10.5	8.65341E-12	0.024099921	-5.91499E-05
131	6.1	-2.65	14	9.04929E-12	0.025307785	-6.2137E-05
132	6.1	-2.65	17.5	9.25182E-12	0.026034541	-6.28848E-05

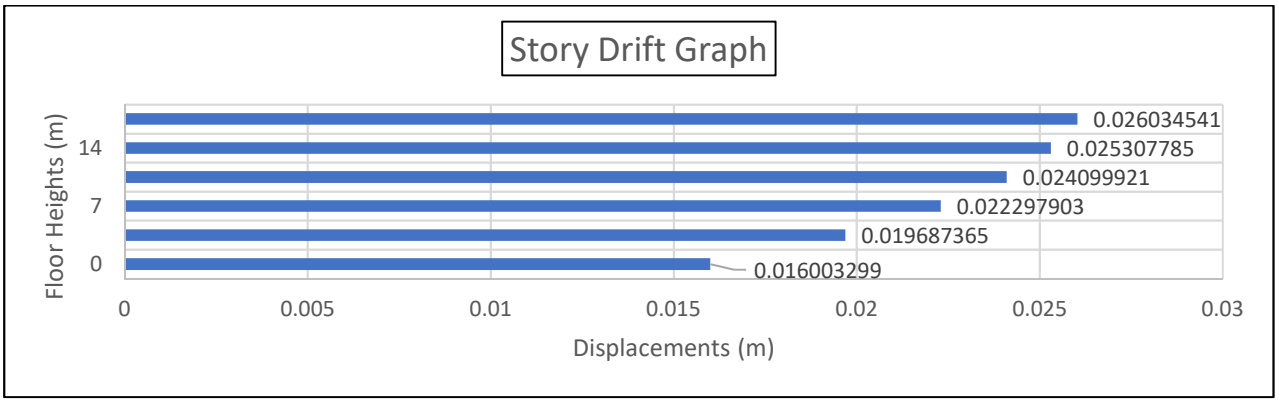

Figure 41: Story Drift Graph of Points on 3-G Axis for F_y = 176.38 kN.

The seventh step is for F_y = 196.38 kN;

Figure 42: Lead Rubber Bearing's hysteresis loop for F_y = 196.38 kN.

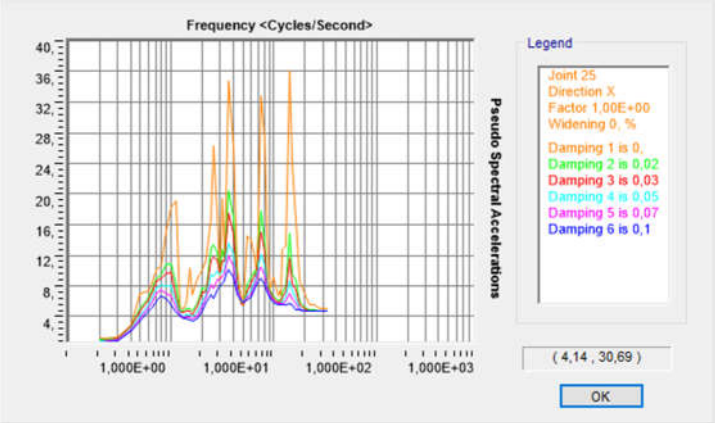

Figure 43: Response spectrum curves for F_y = 196.38 kN.

Table 29: COORDINATES AND DISPLACEMENTS OF POINTS ON 3-G AXIS FOR F_y = 196.38 KN.

Point Number	U1 Coordinates (m)	U2 Coordinates (m)	U3 Coordinates (m)	U1 Displacement (m)	U2 Displacement (m)	U3 Displacement (m)
127	6.1	-2.65	0	4.67134E-07	0.016003299	-1.65632E-05
128	6.1	-2.65	3.5	7.21955E-12	0.019687365	-3.8604E-05
129	6.1	-2.65	7	8.07834E-12	0.022297903	-5.22124E-05
130	6.1	-2.65	10.5	8.65341E-12	0.024099921	-5.91499E-05
131	6.1	-2.65	14	9.04929E-12	0.025307785	-6.2137E-05
132	6.1	-2.65	17.5	9.25182E-12	0.026034541	-6.28848E-05

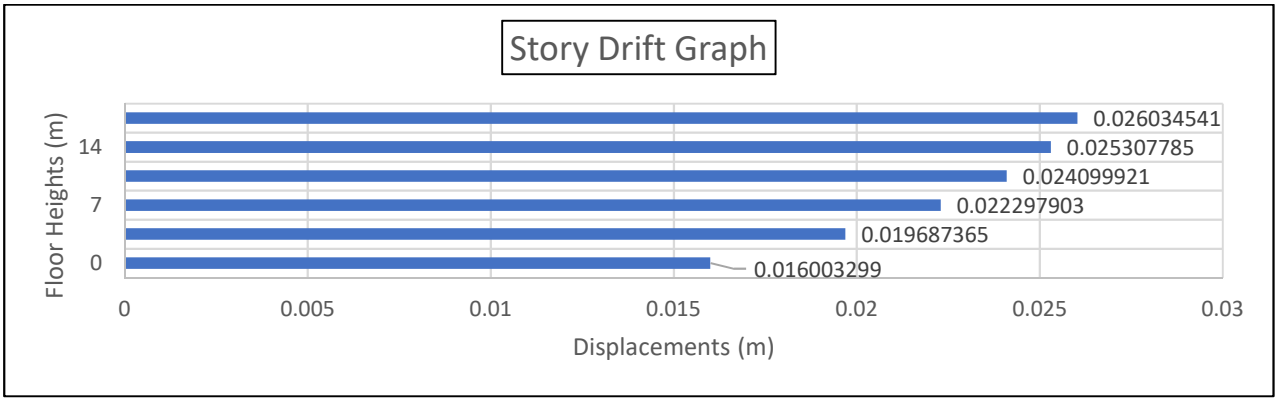

Figure 44: Story Drift Graph of Points on 3-G Axis for F_y = 196.38 kN.

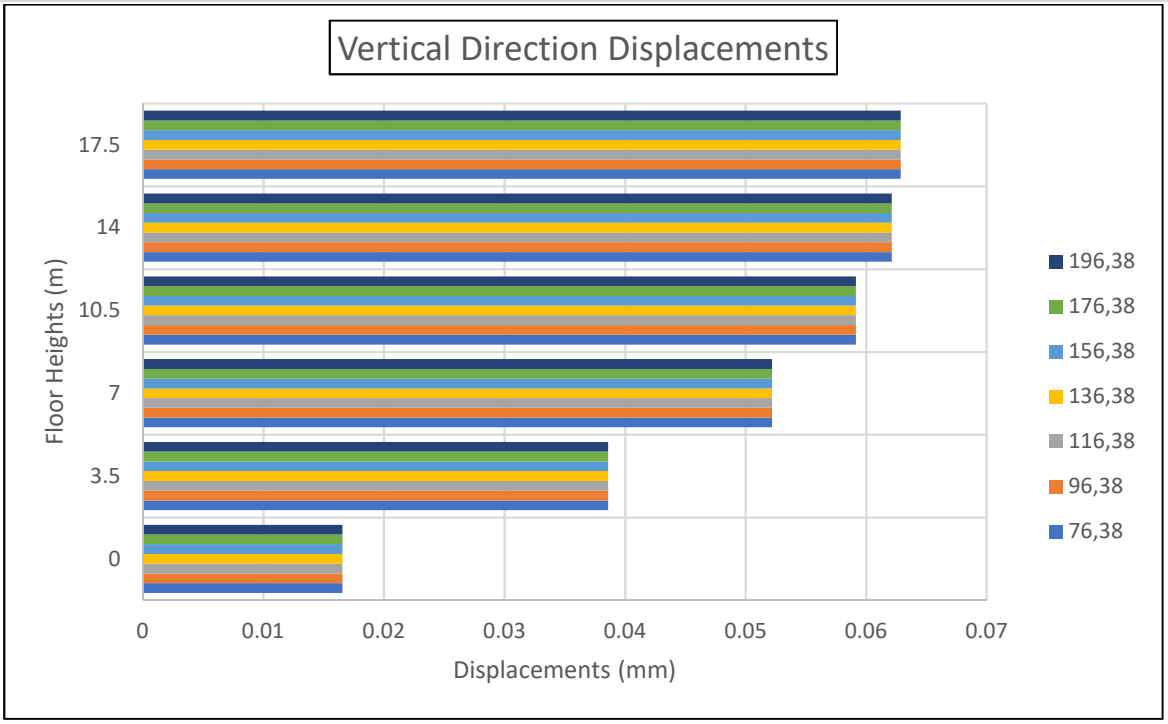

Figure 45: Effect of parameter, yield strength on vertical displacement of the structure.

Parameter Iteration Module – Monitoring the Increment of the Calculated K_H Parameter in Lead Rubber Bearing Type Isolator Model

The initial value for K_H, one of the isolator parameters, was determined as 1482.87 kN/m in the calculations. The limit of the iteration is considered as 2500 kN/m and the increment value as 200.

Table 30: EFFECTIVE STIFFNESS (U2-3) – INCREMENT VALUES FOR K_H PARAMETER

Parameter	Effective Stiffness (U2-3) – K_H
First Step	1482.87 kN/m
Last Step	2482.87 kN/m
Number of Steps	6
Step Range	200 kN/m

The first step is for K_H = 1482.87 kN/m;

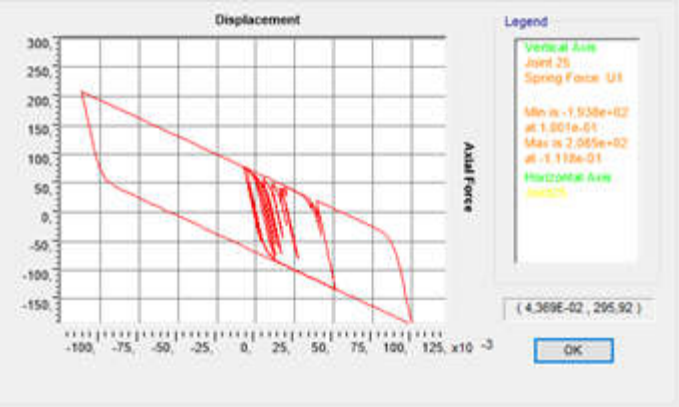

Figure 46*:* Lead Rubber Bearing's hysteresis loop for K_H = 1482.87 kN/m.

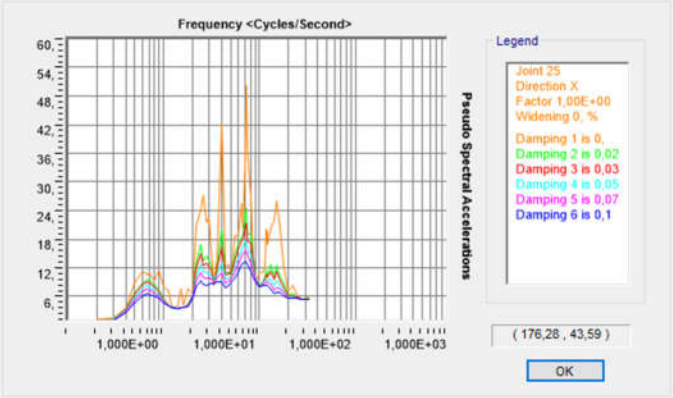

Figure 47: Response spectrum curves for K_H = 1482.87 kN/m.

Table 31: COORDINATES AND DISPLACEMENTS OF POINTS ON 3-G AXIS CURVES FOR K_H = 1482.87 KN/M.

Point Number	U1 Coordinates (m)	U2 Coordinates (m)	U3 Coordinates (m)	U1 Displacement (m)	U2 Displacement (m)	U3 Displacement (m)
127	6.1	-2.65	0	4.67134E-07	0.016003299	-1.65632E-05
128	6.1	-2.65	3.5	7.21955E-12	0.019687365	-3.8604E-05
129	6.1	-2.65	7	8.07834E-12	0.022297903	-5.22124E-05
130	6.1	-2.65	10.5	8.65341E-12	0.024099921	-5.91499E-05
131	6.1	-2.65	14	9.04929E-12	0.025307785	-6.2137E-05
132	6.1	-2.65	17.5	9.25182E-12	0.026034541	-6.28848E-05

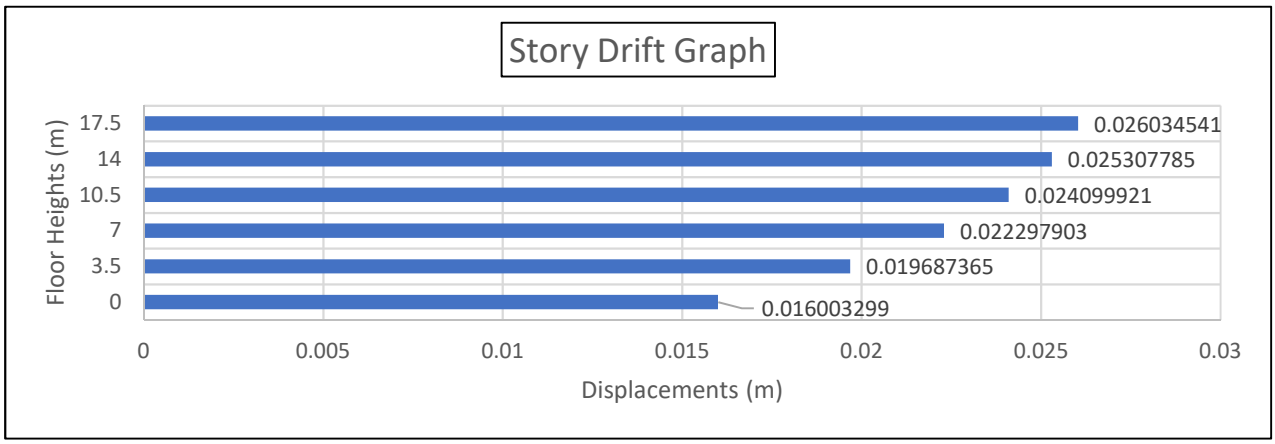

Figure 48: Story Drift Graph of Points On 3-G Axis for effective stiffness (U2-3) = 1482.87 kN/m.

The second step is for K_H = 1682.87 kN/m;

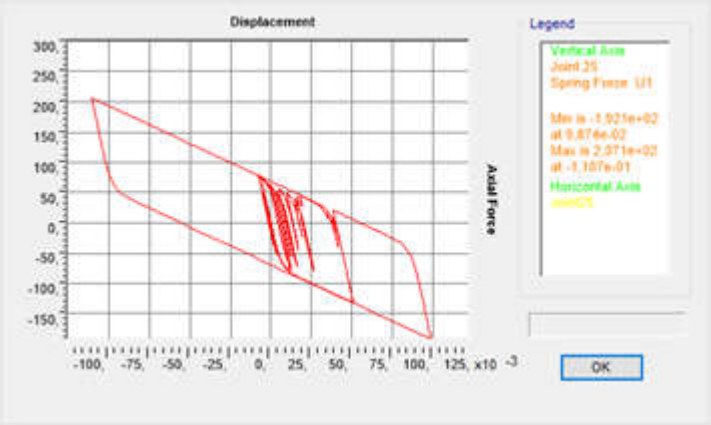

Figure 49: Lead Rubber Bearing's hysteresis loop for K_H = 1682.87 kN/m.

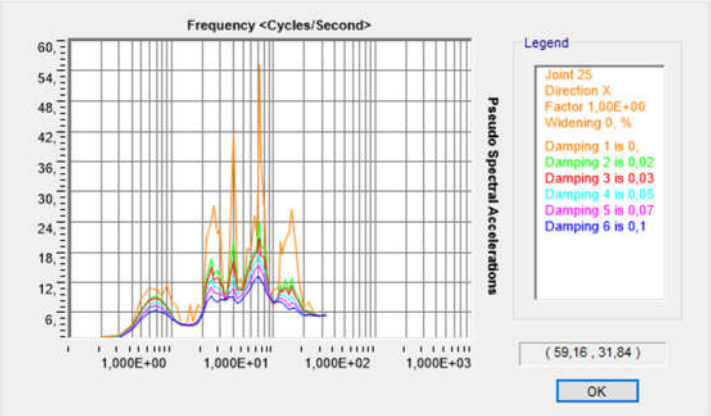

Figure 50: Response spectrum curves for K_H = 1682.87 kN/m.

Table 32: COORDINATES AND DISPLACEMENTS OF POINTS ON 3-G AXIS CURVES FOR K_H = 1682.87 KN/M.

Point Number	U1 Coordinates (m)	U2 Coordinates (m)	U3 Coordinates (m)	U1 Displacement (m)	U2 Displacement (m)	U3 Displacement (m)
127	6.1	-2.65	0	-4.98525E-07	0.015337847	1.80554E-05
128	6.1	-2.65	3.5	-6.15735E-12	0.019347156	4.20818E-05
129	6.1	-2.65	7	-6.9761E-12	0.022187573	5.69261E-05
130	6.1	-2.65	10.5	-7.52946E-12	0.024152433	6.45091E-05
131	6.1	-2.65	14	-7.92399E-12	0.025471645	6.77786E-05
132	6.1	-2.65	17.5	-8.12177E-12	0.026266196	6.85989E-05

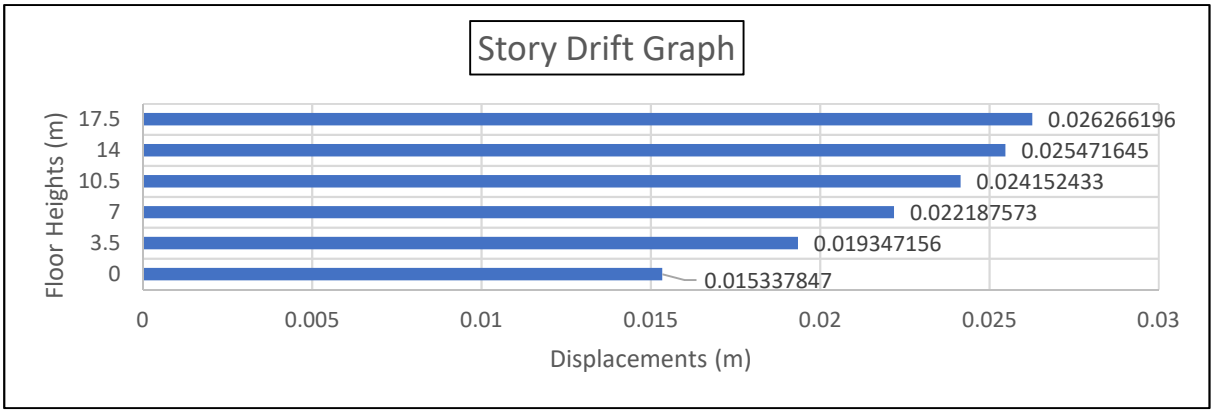

Figure 51: Story Drift Graph of Points on 3-G Axis for K_H = 1682.87 kN/m.

The thrid step is for K_H = 1882.87 kN/m;

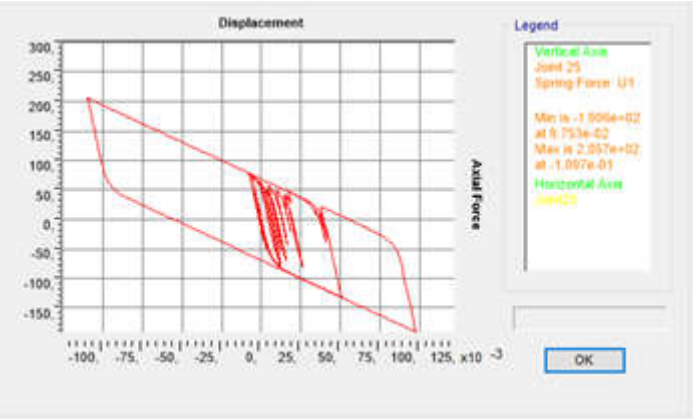

Figure 52: Lead Rubber Bearing's hysteresis loop for K_H = 1882.87 kN/m.

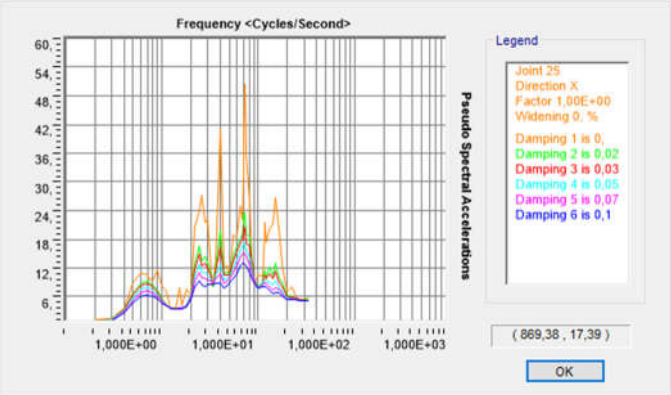

Figure 53: Lead Rubber Bearing's hysteresis loop for K_H = 1882.87 kN/m.

Table 33: COORDINATES AND DISPLACEMENTS OF POINTS ON 3-G AXIS CURVES FOR K_H = 1882.87 KN/M.

Point Number	U1 Coordinates (m)	U2 Coordinates (m)	U3 Coordinates (m)	U1 Displacement (m)	U2 Displacement (m)	U3 Displacement (m)
127	6.1	-2.65	0	-5.2546E-07	0.014724027	1.94296E-05
128	6.1	-2.65	3.5	-5.80245E-12	0.019032169	4.52847E-05
129	6.1	-2.65	7	-6.64791E-12	0.022083466	6.1268E-05
130	6.1	-2.65	10.5	-7.21207E-12	0.024198315	6.94482E-05
131	6.1	-2.65	14	-7.60962E-12	0.025620401	7.29796E-05
132	6.1	-2.65	17.5	-7.79667E-12	0.0264777	7.38675E-05

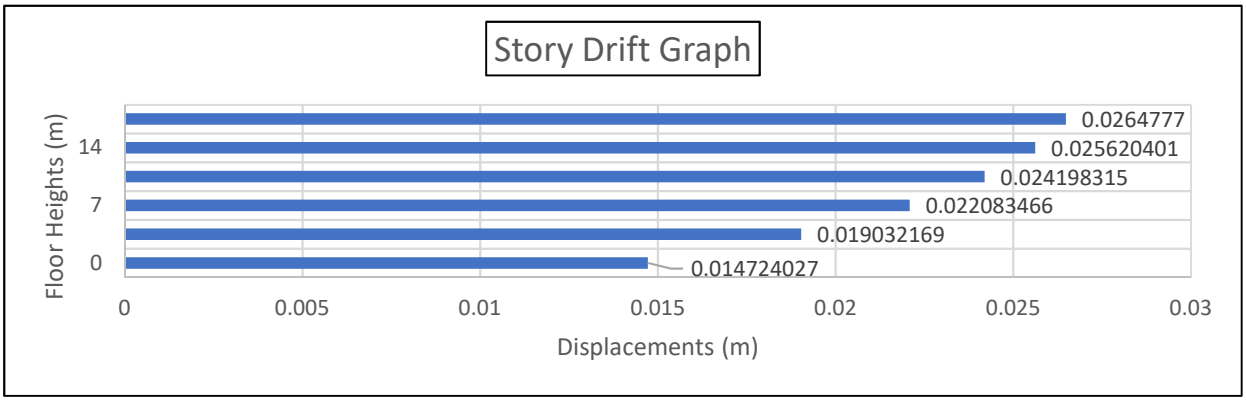

Figure 54: Story Drift Graph of Points on 3-G Axis for K_H = 1882.87 kN/m.

The fourth step is for K_H = 2082.87 kN/m;

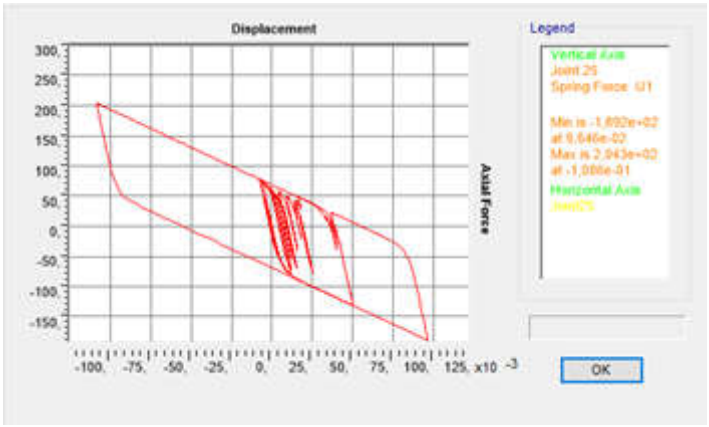

Figure 55: Lead Rubber Bearing's hysteresis loop for K_H = 2082.87 kN/m.

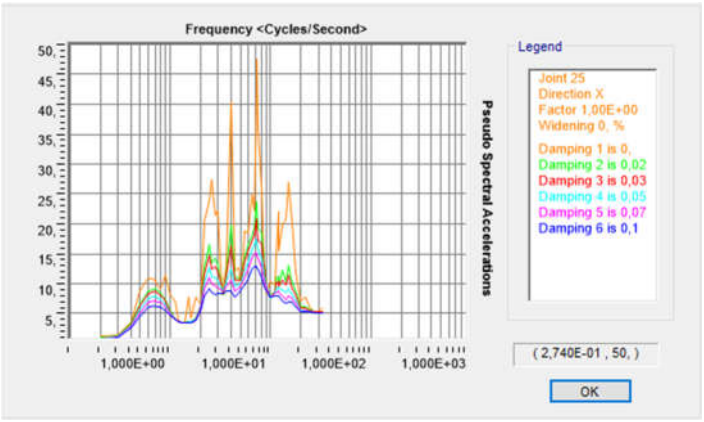

Figure 56: Response spectrum curves for K_H = 2082.87 kN/m.

Table 34: COORDINATES AND DISPLACEMENTS OF POINTS ON 3-G AXIS CURVES FOR K_H = 2082.87 KN/M.

Point Number	U1 Coordinates (m)	U2 Coordinates (m)	U3 Coordinates (m)	U1 Displacement (m)	U2 Displacement (m)	U3 Displacement (m)
127	6.1	-2.65	0	5.48541E-07	0.014156375	-2.06986E-05
128	6.1	-2.65	3.5	3.96923E-12	0.018739924	-4.82423E-05
129	6.1	-2.65	7	4.58472E-12	0.021985217	-6.52777E-05
130	6.1	-2.65	10.5	4.99071E-12	0.024238571	-7.40116E-05
131	6.1	-2.65	14	5.29054E-12	0.025755917	-7.77865E-05
132	6.1	-2.65	17.5	5.41569E-12	0.026671415	-7.87372E-05

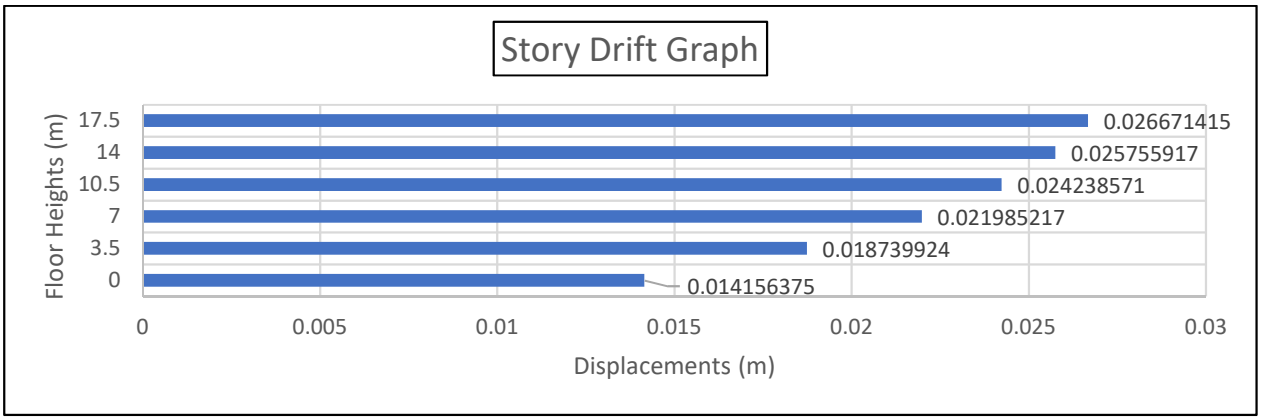

Figure 57: Story Drift Graph of Points on 3-G Axis for K_H = 2082.87 kN/m.

The fifth step is for K_H = 2282.87 kN/m;

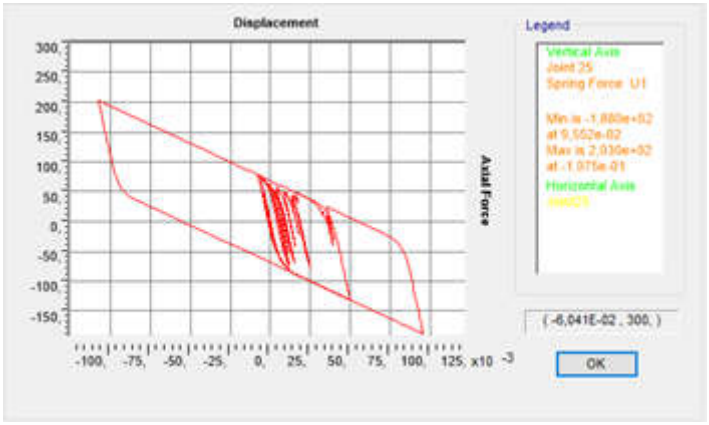

Figure 58: Lead Rubber Bearing's hysteresis loop for K_H = 2282.87 kN/m.

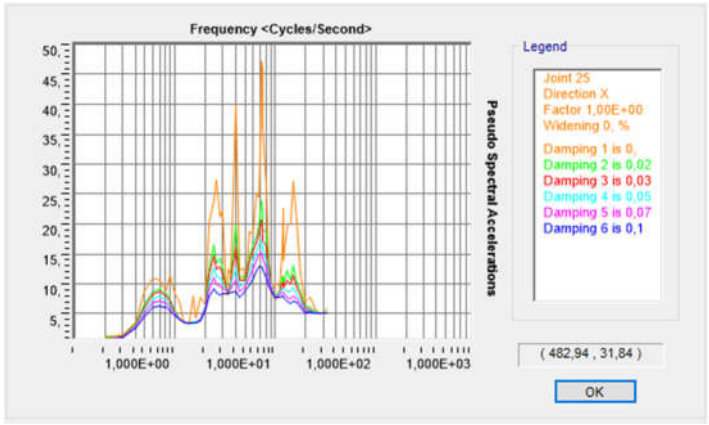

Figure 59: Response spectrum curves for K_H = 2282.87 kN/m.

Table 35: COORDINATES AND DISPLACEMENTS OF POINTS ON 3-G AXIS CURVES FOR K_H = 2282.87 KN/M.

Point Number	U1 Coordinates (m)	U2 Coordinates (m)	U3 Coordinates (m)	U1 Displacement (m)	U2 Displacement (m)	U3 Displacement (m)
127	6.1	-2.65	0	-5.68282E-07	0.013630116	2.18733E-05
128	6.1	-2.65	3.5	-3.46516E-12	0.018468216	5.09801E-05
129	6.1	-2.65	7	-4.04515E-12	0.021892462	6.899E-05
130	6.1	-2.65	10.5	-4.42694E-12	0.024274027	7.82383E-05
131	6.1	-2.65	14	-4.71573E-12	0.025879779	8.22398E-05
132	6.1	-2.65	17.5	-4.82326E-12	0.026849372	8.32493E-05

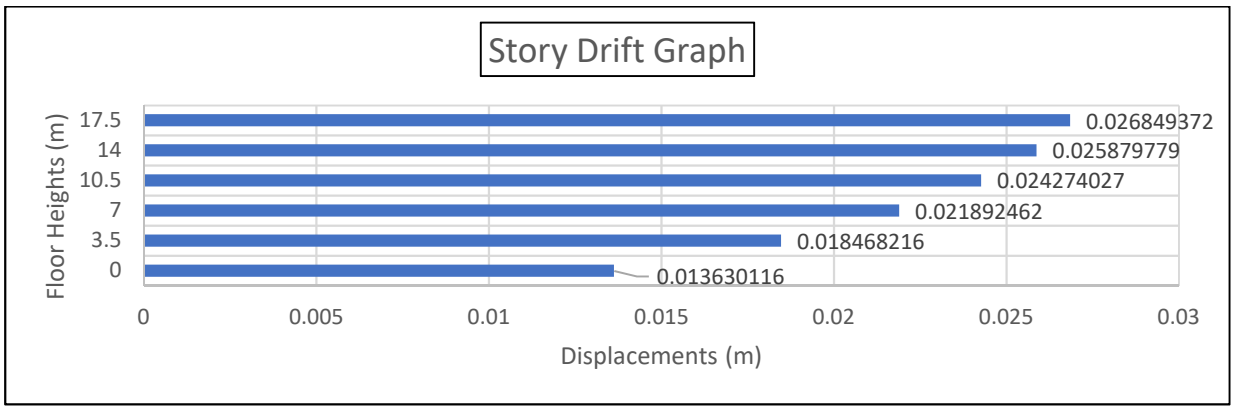

Figure 60: Story Drift Graph of Points on 3-G Axis for K_H = 2282.87 kN/m.

The sixth step is for K_H = 2482.87 kN/m;

Figure 61: Lead Rubber Bearing's hysteresis loop for K_H = 2482.87 kN/m.

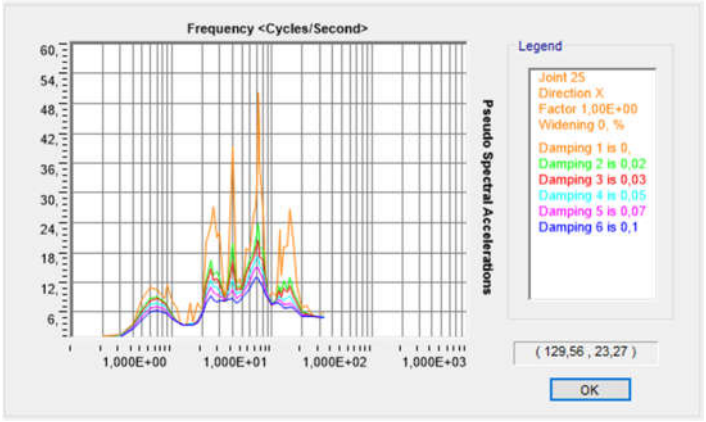

Figure 62: Response spectrum curves for K_H = 2482.87 kN/m.

Table 36: COORDINATES AND DISPLACEMENTS OF POINTS ON 3-G AXIS CURVES FOR K_H = 2482.87 KN/M.

Point Number	U1 Coordinates (m)	U2 Coordinates (m)	U3 Coordinates (m)	U1 Displacement (m)	U2 Displacement (m)	U3 Displacement (m)
127	6.1	-2.65	0	-5.85119E-07	0.013141071	2.29634E-05
128	6.1	-2.65	3.5	-3.14351E-12	0.018215095	5.35208E-05
129	6.1	-2.65	7	-3.70863E-12	0.021804845	7.24352E-05
130	6.1	-2.65	10.5	-4.08172E-12	0.024305372	8.21624E-05
131	6.1	-2.65	14	-4.36954E-12	0.025993347	8.63751E-05
132	6.1	-2.65	17.5	-4.47295E-12	0.02701332	8.74396E-05

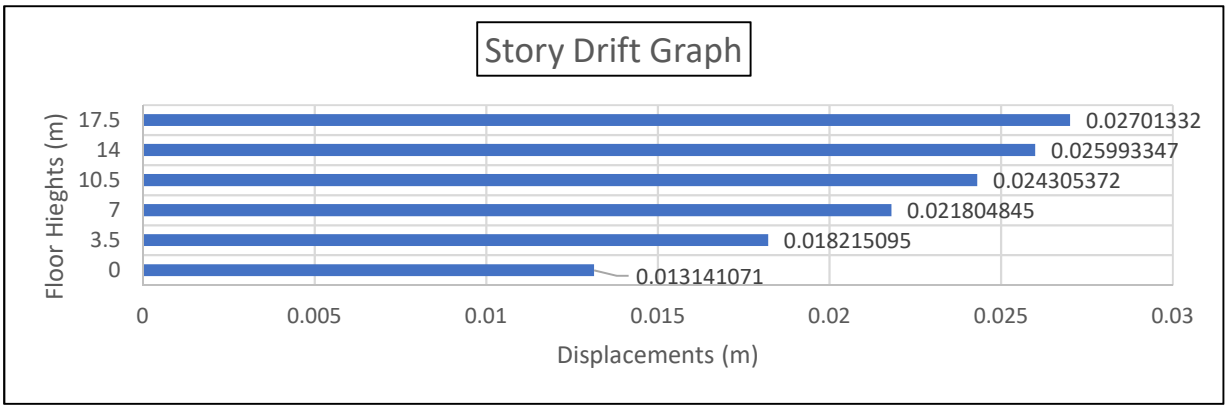

Figure 63: Story Drift Graph of Points on 3-G Axis for K_H = 2482.87 kN/m.

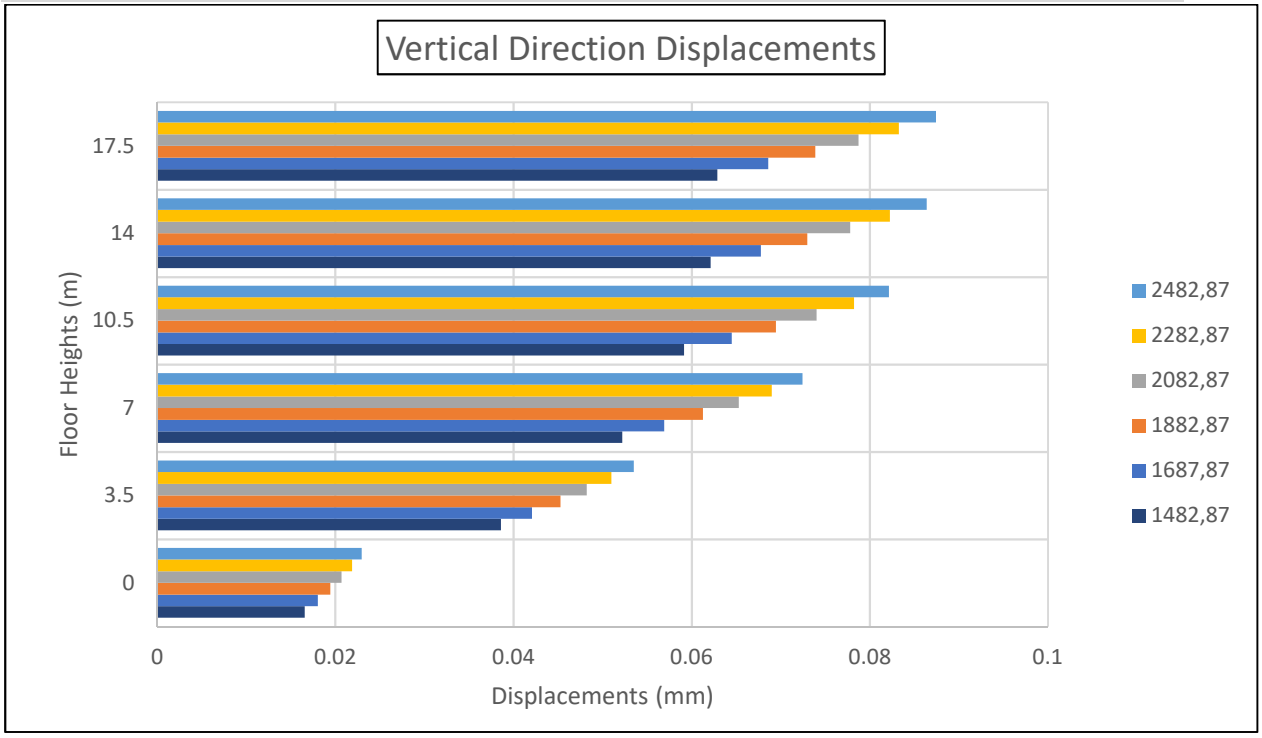

Figure 64: Effect of parameter. K_H on vertical displacement of the structure.

Conclusion

Seismic isolators play a major role in reducing the harmful effects of earthquakes. It is important that the properties of seismic isolators should be selected at correct values in order to reduce these effects appropriately. For this purpose, parametric analysis is one of the leading options in determining the required properties of isolators under the influence of complex behaviors of a structural system. Analyzes made in accordance with the UBC-97 code, the effects of changes in the properties of the LRB type isolator on the structures were carried out using the SAP2000 and OAPI interface of SAP2000.

It has been observed that there is no significant change in the horizontal displacements of the structure due to the increases in the inspection interval of the K_V parameter, which is one of the parameters examined for isolator design and analysis. The vertical displacement values decreased considerably with the increase of the K_V parameter.

A significant effect of the value increases in the integrated yield strength, another study parameter, on the horizontal and vertical displacements of the structure has not been observed. However, the shape of the hysteresis curve created for the isolator has shown a significant change in behavior depending on the integrated yield strength. When the changes of the hysteresis curve are examined, it shows that the damping of the axial loads on the isolators due to the increasing values of the integrated yield strength within the operating range is achieved with decreasing displacement values.

The effect of the value change in the K_H parameter on the horizontal displacements of the structure does not have a proportional and unchanging form. While the deflections in certain parts of the building decrease due to the change in K_H, the deflections in other parts may increase.

By using the parameters of the LRB isolators, the effects of isolators with different properties on the behavior of the structures were investigated using a structural analysis program. In the study, a script specially prepared for this study was used to manage the parametric analysis of the effects of changes in the properties of the isolators on structural behavior. Thanks to the script that has been prepared, it is not only possible to perform the work, but also there is no need to use a GUI for value entries and result readings. Since the GUI is not used, it has become possible to perform analyzes much faster than if the analysis is done in classical routine.

By means of the script prepared for this study, it has become possible not only to analyze specific analyzes for this study, but also to make analyzes according to different scenarios related to the subject, determination of suitable isolators and analysis of their effects on the structure.

REFERENCES

Application Programming Interface | Computers and Structures, Inc. [WWW Document], n.d. URL https://www.csiamerica.com/application-programming-interface (accessed 6.24.20).

Constantinou, M., Whittaker, A., Yanni Kalpakidis, Fenz, D., Warn, G., 2007. Performance of seismic isolation hardware under service and seismic loading. https://doi.org/10.13140/RG.2.1.4633.8166

Güner, G., 2012. Bir Hastane Yapısının Klasik Yöntemle Ve Sismik İzolatör Kullanılarak Tasarımının Dinamik Yönden Karşılaştırılmasının Yapılması (Thesis). Fen Bilimleri Enstitüsü.

Kelly, J.M., 2004. Seismic isolation, in: Earthquake Engineering. CRC Press, pp. 692–731.

Kelly, T.E., 2001. Base isolation of structures: Design guidelines. Wellington, New Zealand: Holmes Consulting Group Ltd.

Lutz, M., 2017. Programming Python, Fourth edition. ed. O'Reilly, Beijing Bosotn Farnham Sebastopol Tokyo.

Robinson, W.H., Tucker, A.G., 1983. Test results for lead-rubber bearings for WM. Clayton building, Toe Toe bridge and Waiotukupuna bridge. Bulletin of the New Zealand National Society for Earthquake Engineering 14, 21–33.

Robinson, W.H., Tucker, A.G., 1977. A lead-rubber shear damper. Bull. New Zealand Natl. Soc. Earthquake Engrg 4, 251–59.

Skinner, R.I., Robinson, W.H., McVerry, G.H., 1993. An introduction to seismic isolation. Wiley, Chichester ; New York.

Uniform Building Code, 1997. UBC-97, in: Structural Engineering Design Provisions. International Conference of Building Officials, Whittier, California.

What is Python? Executive Summary [WWW Document], n.d. . Python.org. URL https://www.python.org/doc/essays/blurb/ (accessed 12.29.19).

MCBU CIVIL ENGINEERING REPORTS

MCBUCIVILENG.R-2020.1

Parametric Design and Investigation of Base Isolators Using the Script Developed on SAP2000 OAPI

Oğuzhan Usta
Gökhan Altıntaş

MCBU
Engineering Faculty
Civil Engineering Department
https://civilengineering.mcbu.edu.tr

SCIENCE + TECHNOLOGY